

# The Star Formation History of WLM from Asymptotic Giant Branch Stars and The Discovery of a Possible Accreted System in its Outer Disk

ABIGAIL J. LEE,<sup>1,\*</sup> DANIEL R. WEISZ,<sup>1</sup> ANDREW E. DOLPHIN,<sup>2,3</sup> AND ALESSANDRO SAVINO<sup>1</sup>

<sup>1</sup>*Department of Astronomy, University of California, Berkeley, CA 94720-3411, USA*

<sup>2</sup>*Raytheon, 1151 E. Hermans Road, Tucson, AZ 85756, USA*

<sup>3</sup>*Steward Observatory, University of Arizona, 933 N. Cherry Avenue, Tucson, AZ 85719, USA*

## ABSTRACT

We measure the star formation history of Local Group dwarf galaxy WLM using wide-area ( $\sim 4$  half-light radii) ground-based NIR imaging of bright ( $M_J < -4.9$  mag) asymptotic giant branch (AGB) stars. From our NIR color-magnitude diagram (CMD) of 825 stars, we find that our recovered SFH is in excellent agreement with literature SFHs of WLM measured from much deeper CMDs ( $M_{F090W} \sim +4.3$  mag) based on James Webb Space Telescope (JWST) imaging. We find good agreement in the qualitative shape of the SFHs as well as quantitative metrics such as the timescales for which 50% and 90% of the stellar mass formed with  $\tau_{50,AGB} = 5.16^{+2.07}_{-0.50}$  Gyr ago and  $\tau_{90,AGB} = 1.33^{+0.11}_{-0.09}$  Gyr ago versus  $\tau_{50,JWST} = 5.29^{+0.34}_{-0.28}$  Gyr ago and  $\tau_{90,JWST} = 1.42^{+0.16}_{-0.01}$  Gyr ago. The coarser precision of the AGB star-based values is driven by the low number of AGB stars. We also recover an age gradient that is in good agreement with the age gradient measured from JWST data, where we find the outer regions of WLM are on average older than the inner regions. We derive an age-metallicity relation (AMR) from the AGB star CMD fitting that is similar to the JWST-based AMR and is consistent with other reported metallicities in WLM (i.e., spectroscopy, RR Lyrae). From our wide-area AGB star map and SFH, we identify a stellar over-density ( $M_* \sim 2.0 \times 10^6 M_\odot$ ,  $r_h \sim 340$  pc) in WLM's northwestern outer disk. The over-density's SFH shows a burst of star formation  $\sim 8$  Gyr ago and its spatial location is near a known warp in WLM's H I. Despite WLM having long been considered an isolated galaxy, the mass, size, and age of this over-density are highly suggestive of an accreted dwarf galaxy. Overall, our findings illustrate the power of NIR observations of AGB stars for efficiently and accurately measuring SFHs and for identifying and characterizing substructures in nearby galaxies.

*Keywords:* Asymptotic giant branch (108), Galaxy stellar content (621), Hertzsprung Russell diagram (725), Near infrared astronomy (1093), Stellar populations (1622), Asymptotic giant branch stars (2100)

## 1. INTRODUCTION

Color-magnitude diagrams (CMDs) that extend below the oldest main sequence turnoff (oMSTO) are the ‘gold standard’ for measuring a galaxy’s star formation history across cosmic time (e.g., M. L. Mateo 1998; C. Gallart et al. 2005; E. Tolstoy et al. 2009; R. C. Kennicutt & N. J. Evans 2012; C. Conroy 2013). Unfortunately, due to the crowding and faintness of the oMSTO ( $M_V \sim +4$ ), even the Hubble Space Telescope (HST) has only been able to reach the oMSTO in galaxies

within the Local Group (LG). While these SFHs measured from the oMSTO have had high-scientific impact, particularly on our knowledge of low-mass galaxies (e.g., J. Harris & D. Zaritsky 2004, 2009; A. A. Cole et al. 2007; M. Monelli et al. 2010a,b; S. L. Hidalgo et al. 2011, 2013; T. M. Brown et al. 2014; E. D. Skillman et al. 2014, 2017; D. R. Weisz et al. 2014a; C. Gallart et al. 2015; S. Rubele et al. 2015, 2018; A. Mazzi et al. 2021; E. Sacchi et al. 2021; A. Savino et al. 2023, 2025; M. J. Durbin et al. 2025), they have been inherently limited to the LG, which has a specific accretion history that may not be representative of the broader Universe. The James Webb Space Telescope (JWST) has produced the first CMD that reached the oMSTO just outside the LG (Leo P;  $D \sim 1.6$  Mpc; K. B. W. McQuinn et al. 2024a). But

Corresponding author: Abigail J. Lee  
abby.lee@berkeley.edu

\* NASA Hubble Fellow

even with its excellent angular resolution and sensitivity, crowding and faintness will limit JWST observations of the oMSTO to distances of  $\sim 2 - 3$  Mpc.

Extending CMD-based SFHs to environments well-beyond the LG has and will continue to rely on evolved stars (e.g., S. M. Gogarten et al. 2010; B. F. Williams et al. 2009, 2010; K. B. W. McQuinn et al. 2010a,b; D. R. Weisz et al. 2011; M. Cignoni et al. 2018, 2019; E. Sacchi et al. 2018, 2019; A. Smercina et al. 2025). Typically, in the optical, CMD features such as the subgiant branch (SGB;  $M_V \sim +3.5$ ), the horizontal branch (HB;  $M_V \sim +0.5$ ), and red clump (RC;  $M_V \sim +0.5$ ) are considered the next-best features on the CMD for measuring lifetime SFHs (e.g., C. Gallart et al. 2005). The oldest SGB is almost as faint as the oMSTO and provides only marginally better observational prospects (e.g., A. A. Cole et al. 2014). The HB is known to be highly sensitive to age (e.g., A. Savino et al. 2019), but HB-based SFHs can be limited in precision by the small number of HB stars available and are highly dependent on the choice in stellar model (e.g., C. Gallart et al. 2005). In principle, accurately modeling the HB on CMDs should include variations in more complex stellar physics (e.g., mass loss; A. Savino et al. 2019).

RC-depth CMDs have long been the target of resolved star observations in nearby galaxies as they provide a balance of realistic observational considerations and age-sensitivity (e.g., D. R. Weisz et al. 2008; B. F. Williams et al. 2009, 2017; K. B. W. McQuinn et al. 2010a; D. R. Weisz et al. 2011, 2014a; A. Smercina et al. 2025). In principle, the RC consists of core helium-burning stars with ages between  $\sim 1 - 10$  Gyr, which can provide age information. However, the effects of stellar evolution tend to skew the RC age distribution toward younger ( $\sim 1 - 4$  Gyr) and metal-rich populations (e.g., C. Gallart et al. 2005; L. Girardi 2016). It is also a phase of evolution known for its complexity; uncertainties in core overshooting, rotation, binarity, and mass loss can be significant and are only marginally calibrated (e.g., L. Girardi 2016). In practice, age information based on RC-depth CMDs is more tightly constrained by the ratio of RC to red giant branch (RGB) stars. While SFHs measured from RC-depth CMD have been shown to be accurate, they only provide coarse time resolution at lookback times older than a few Gyr (e.g., D. R. Weisz et al. 2014a).

An emerging alternative for measuring SFHs in galaxies beyond the LG are asymptotic giant branch (AGB) stars. AGB stars are evolved intermediate and low-mass stars ( $0.5 - 8M_\odot$ ) near the end of their lifetimes. AGB stars are known to be sensitive to age and are significantly brighter than other age-sensitive CMD features

(e.g., J. A. Frogel & V. M. Blanco 1983; N. Reid & J. Mould 1984; P. R. Wood et al. 1985; E. Costa & J. A. Frogel 1996; T. J. Davidge 2003, 2005, 2014; M.-R. L. Cioni & H. J. Habing 2005; J. Melbourne et al. 2010; M. Y. Jung et al. 2012; D. Crnojević et al. 2013; K. B. W. McQuinn et al. 2017). Their potential for SFH measurements has been recognized for decades (e.g., C. Gallart et al. 1996; M.-R. L. Cioni et al. 2006a,b, 2008; E. V. Held et al. 2010; A. Javadi et al. 2011a; M. Rejkuba et al. 2022; B. Harmsen et al. 2023; B. N. Velguth et al. 2024).

However, two challenges have limited the practical use of AGB stars for SFH measurements. First, AGB stars are less age-sensitive in optical wavelengths (A. Javadi et al. 2011b; A. J. Lee et al. 2025). Furthermore,  $\sim 40\%$  of AGB stars, particularly the metal-rich and cool AGB stars, are undetected in optical wavelengths (A. A. Zijlstra et al. 1996; D. C. Jackson et al. 2007; M. L. Boyer et al. 2009, 2019; E. V. Held et al. 2010). This ultimately has limited the utility of AGB star SFHs for the wealth of optical CMDs in the literature (e.g., J. A. Holtzman et al. 2006; J. J. Dalcanton et al. 2009). Second, AGB stars exhibit a variety of complex physics (e.g., mass loss, dredge up, thermal pulses, self-extinction) that can limit the accuracy of age information (L. Girardi et al. 2010; P. Marigo et al. 2017), indicating that careful calibration of any age from information from AGB stars is required.

Over the past decade, there have been two significant advances that changed the landscape for AGB star SFHs. First, AGB stars ages in new stellar models developed in the past several years by the COLIBRI group (P. Marigo et al. 2017; G. Pastorelli et al. 2019, 2020) have been anchored to SFHs measured from the oMSTO in the Magellanic Clouds (S. Rubele et al. 2018; A. Mazzi et al. 2021). This places AGB star based ages on a self-consistent scale with MSTO stars when used in CMD modeling. Second, is the increasing abundance of NIR imaging in nearby galaxies. It is only at near-infrared (NIR) wavelengths that C-type AGB, M-type AGB, and RGB stars cleanly separate (e.g., S. Nikolaev & M. D. Weinberg 2000; M.-R. L. Cioni & H. J. Habing 2003; T. J. Davidge 2003, 2005; A. Kang et al. 2005; Y.-J. Sohn et al. 2006; D. C. Jackson et al. 2007; A. T. Valcheva et al. 2007; M. L. Boyer et al. 2009, 2019; E. V. Held et al. 2010; M. Y. Jung et al. 2012; A. J. Lee et al. 2025), allowing exclusively for AGB star based SFHs. NIR imaging of resolved AGB stars will be easily acquired in the upcoming years with facilities such as JWST, Roman, and Euclid, providing a platform for measuring SFHs from resolved AGB stars.

In [A. J. Lee et al. 2025](#) (hereafter [L25](#)), we established that the SFH of M31’s disk measured only from modeling AGB stars on NIR CMDs is consistent with M31’s SFH measured from optical CMDs that reach below the RC from [B. F. Williams et al. \(2017\)](#). Though an important result on its own, it would be better to validate SFHs based on AGB stars against SFHs measured from CMDs that reach the oMSTO. This is challenging because such a comparison needs to fulfill several criteria. First, it requires a dataset that contains enough AGB stars to measure an accurate SFH. [L25](#) found that at least  $\sim 1000$  stars on a NIR CMD are required to measure an accurate SFH (this includes AGB stars, RHeB stars, and bright RGB stars). Second, the NIR CMD needs to extend  $\gtrsim 1$  mag below the TRGB. Finally, the galaxy needs to have an optical or NIR CMD that reaches below the oMSTO for validation over a similar area as the NIR data. Most available datasets fail to simultaneously fulfill these criteria. The Magellanic Clouds do satisfy these criteria. However, they were used to calibrate the COLIBRI AGB star models and cannot also be used for validation. M31 and M33 contain large numbers of AGB stars but lack oMSTO-derived SFHs or have oMSTO-based SFH over very small areas (e.g., [T. M. Brown et al. 2006](#); [J. C. Richardson et al. 2008](#); [E. J. Bernard et al. 2015](#)). Galaxies with oMSTO-derived SFHs, such as dwarf galaxies (e.g., [M. Gullieuszik et al. 2007a,b, 2008a,b](#); [J. Menzies et al. 2008](#); [E. V. Held et al. 2010](#); [A. Savino et al. 2025](#)) or galaxies with SFHs derived from small-area HST or JWST fields (e.g., [A. E. Dolphin et al. 2003](#); [E. D. Skillman et al. 2003](#); [T. J. L. de Boer et al. 2011, 2012a,b, 2014](#); [M. Geha et al. 2015](#); [R. R. Muñoz et al. 2018](#)), typically lack sufficient numbers of AGB stars.

One galaxy that approximately satisfies these criteria is WLM. WLM is a star-forming dwarf galaxy ( $M_\star = 4.3 \times 10^7 M_\odot$ ; [A. W. McConnachie 2012](#)) located at the edge of the Local Group ( $d = 986$  kpc; [A. J. Lee et al. 2021](#)). WLM is often considered an archetypal ‘isolated’ dwarf galaxy (i.e., its evolution has not been shaped by significant interactions with a more massive galaxy).

WLM’s SFH has been measured from the oMSTO from multiple HST and JWST fields ([S. M. Albers et al. 2019](#); [K. B. W. McQuinn et al. 2024b](#); [R. E. Cohen et al. 2025](#)). There exists separate ground-based NIR photometry of WLM that both extends at least  $\sim 1$  mag below the TRGB and contains a sufficient number of AGB stars to measure an accurate SFH ([A. J. Lee et al. 2021](#)). While these datasets are not perfectly matched spatially, we only need to make modest assumptions about the spatial distribution of the populations to correct for this as we detail later in this paper. We therefore undertake

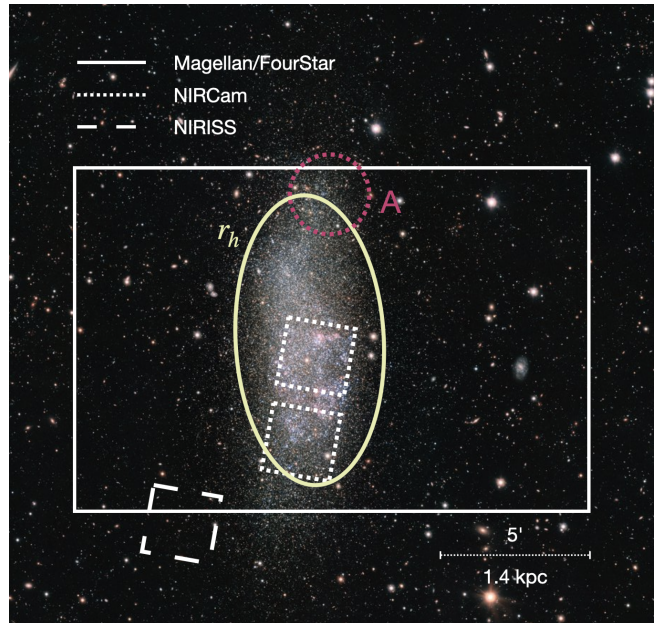


**Figure 1.** Optical image of WLM (image credit: ESO’s VST/Omegacam) overlaid with footprints of the Magellan/FourStar (solid), JWST NIRCcam (dotted), and NIRISS (dashed) fields. The pale yellow line denotes WLM’s half-light radius. The half-light circle of Region ‘A’ is denoted by the pink circle and is discussed in §5.

a comparison of the lifetime SFH of WLM derived from data that reach below the oMSTO and NIR data of only AGB stars.

This paper is organized as follows. We summarize the observations and photometry in §2. The SFH methodology is described in §3. We present our main results and compare our SFHs with those measured from deep JWST imaging in §4. We present the discovery of a potential accreted system in WLM’s outer disk in §5. We discuss radial age and metallicity gradient trends in §6. We discuss the future prospects of using AGB stars as SFH indicators with JWST in §7. We summarize our findings in §8.

## 2. DATA

To measure the AGB star SFH of WLM, we use NIR ground-based imaging taken at the 6.5 m Magellan-Baade telescope at Las Campanas Observatory using the FourStar Infrared Camera ([S. E. Persson et al. 2013](#)) in the  $J$  and  $K_S$  filters. Three sets of observations were taken: two in 2011 with exposures of  $\sim 10^4$  s each and one in 2019 for calibration purposes for  $\sim 10$  seconds. [A. J. Lee et al. \(2021\)](#) previously used these data to measure distances to WLM. Details of the data acquisition and point source fitting photometric reduction can be found in that paper.

Figure 1 shows the footprint of the FourStar field overlaid on an optical image of WLM. This field covers WLM’s entire disk and part of its stellar halo ( $\sim 176 \text{ arcmin}^2/14.5 \text{ kpc}^2$ ), and extends out to  $\sim 4.0r_h$  on the minor axis.

Figure 2 shows our NIR CMD of WLM. Alongside the AGB stars (yellow shading), we indicate the locations of RGB (purple shading) and RHeB stars (red shading). The selection criteria were chosen visually, based on clear features in the CMD, such as the TRGB and the red and blue edges of the RGB. For reference, the signal-to-noise ratio (SNR) of the photometry is  $\approx 85$  at the boundary between the TRGB and the faintest AGB stars ( $J \sim 20$ ).

WLM’s low Galactic latitude results in a non-negligible number of MW foreground stars in our NIR CMD. We identified and removed these foreground stars using *Gaia* data. Specifically, we matched stars from our NIR CMD to sources from the *Gaia* DR3 source catalog (Gaia Collaboration et al. 2016, 2023) and removed matched sources closer than  $1''$  and with colors bluer than  $(J - K) = 0.85 \text{ mag}$ . We selected this color cut based on a simulation of Galactic foreground stars in these filters from TRILEGAL (L. Girardi et al. 2005). The removed MW stars are shown as purple x’s in Figure 2.

To place WLM’s different stellar populations (AGB, RGB, RHeB) into context, we show their spatial distributions in Figure 3. The RGB and AGB populations have qualitatively similar spatial distributions, whereas the RHeB stars are more sparse and centrally concentrated, as is often the case in star-forming dwarf galaxies (e.g., N. Bastian et al. 2011).

WLM was observed with NIRCcam and NIRISS imaging part of the JWST Early Release Science program for Resolved Stellar Populations (D. R. Weisz et al. 2023). We plot footprints of the NIRCcam and NIRISS fields in Figures 1 and 3.

While the JWST data reach well below the oldest MSTO, they only cover a modest fraction of WLM’s total area. The JWST data alone contain too few AGB stars for a robust SFH. Instead, we rely on the oldest MSTO-based SFHs measured from these JWST fields as a comparison point for our AGB star-based SFHs. The JWST observations of WLM were reduced following the procedures outlined by the ERS program (D. R. Weisz et al. 2024). Extensive details of the JWST observations and photometric reductions are provided in K. B. W. McQuinn et al. (2024b) and R. E. Cohen et al. (2025).

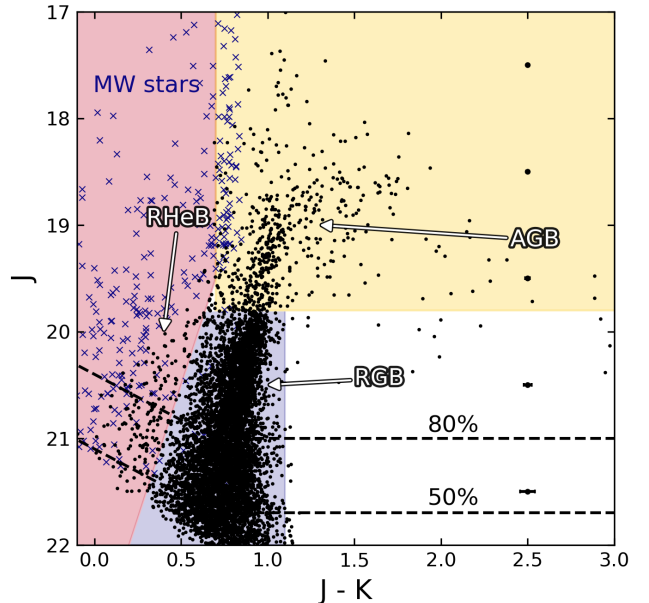


**Figure 2.** Ground-based NIR CMD of WLM which includes  $\sim 13,000$  stars, of which 825 are used in our CMD modeling analysis ( $J < 20 \text{ mag}$ ,  $-0.2 < J - K < 3 \text{ mag}$ ). Representative photometric uncertainties are shown on the right-hand side as a function of magnitude. We indicate AGB stars (yellow shading), RHeB stars (red shading), and RGB stars (purple shading). Spatial maps of these populations are shown in Figure 3. The purple x’s represent stars that were matched with *Gaia* and removed as foreground stars. The 80% and 50% completeness limits are marked with dashed lines. All sources have a signal-to-noise ratio (SNR) of  $\geq 7$  in the J band. Stars at the color and magnitude of the TRGB have an SNR  $\approx 85$  in the J band.

### 3. METHODOLOGY

To measure the AGB star SFH of WLM, we followed the procedure outlined in L25, which we briefly summarize here.

First, we fit the CMD using the CMD-modeling software package MATCH (Version 2.7; A. E. Dolphin 2002, 2012, 2013, 2016). MATCH recovers a system’s SFH by finding the linear combination of synthetic CMDs that best match the observed CMD. We generated custom single stellar population (SSP) models constructed from the COLIBRI AGB stellar isochrones (version S\_37; A. Bressan et al. 2012; J. Tang et al. 2014; Y. Chen et al. 2014, 2015; P. Marigo et al. 2017; G. Pastorelli et al. 2019, 2020). These COLIBRI models were calibrated using observations of AGB stars in the LMC and SMC, the latter of which has a similar metallicity to WLM.

We generated our SSPs using a Kroupa initial mass function (P. Kroupa 2001) normalized between  $0.03M_{\odot}$  and  $120M_{\odot}$  using an SFR of  $0.75 M_{\odot} \text{ yr}^{-1}$ , over an age range of  $6.70 < \log_{10}(t/\text{yr}) < 10.15$  with 0.1 dex

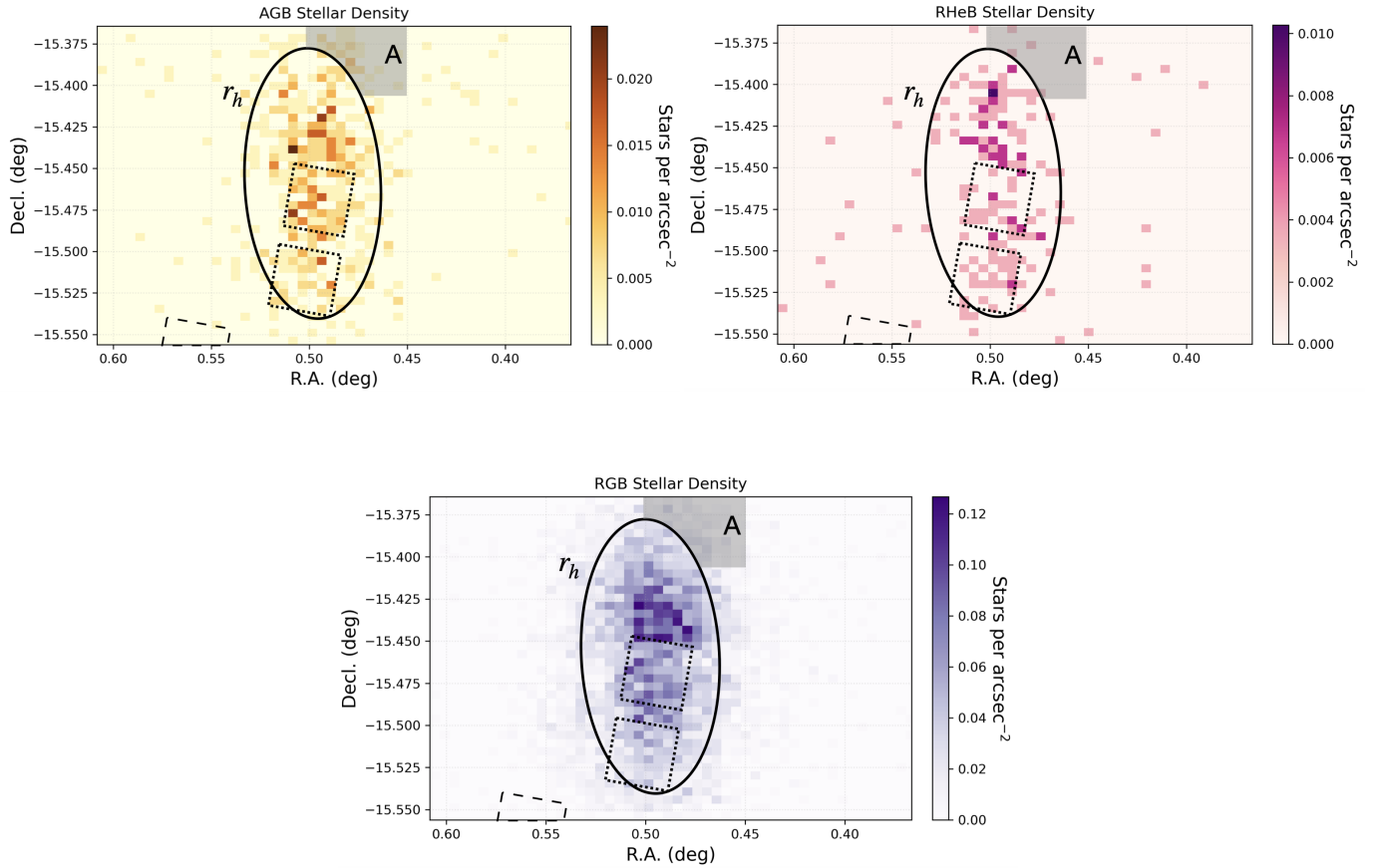


**Figure 3.** The spatial distribution of RGB, AGB, and RHeB stars. The photometric criteria used to select each respective stellar population is shown in Figure 2. The grey highlighted region labeled “A” is discussed in §5.

resolution from  $6.7 < \log_{10}(t/\text{yr}) < 9.0$  and 0.05 dex resolution from  $9.00 < \log_{10}(t/\text{yr}) < 10.15$ . These SSPs spanned metallicities from  $-2.0 \leq [M/H] \leq -0.5$  with a resolution of 0.1 dex. Following common practice in the literature (e.g., D. R. Weisz et al. 2014b; A. Savino et al. 2023; K. B. W. McQuinn et al. 2024b; R. E. Cohen et al. 2025), we required the metallicity to increase monotonically as a function of time (with a spread of 0.1 dex at each age), with a metallicity range of  $-2.0 \leq [M/H] \leq -1.4$  at the oldest time to a present-day metallicity range of  $-1.0 \leq [M/H] \leq -0.5$ .

For the purposes of validation, we chose these metallicity prior ranges to match those of R. E. Cohen et al. 2025 (hereafter C25), who measured WLM’s SFH from the JWST NIRCам and NIRISS data. We did not fix the metallicities or age-metallicity relations (AMRs) to be identical, only the starting and ending ranges. These values are commonly adopted in other LG SFH determinations (e.g., M. Monelli et al. 2010a, 2016; D. R. Weisz et al. 2014b; E. D. Skillman et al. 2017; J. R. Hargis et al.

2020; A. Savino et al. 2023, 2025; K. B. W. McQuinn et al. 2024a,b; R. E. Cohen et al. 2025).

We modeled observational effects in the CMD (photometric errors and incompleteness) using  $3 \times 10^4$  artificial star tests (ASTs). The ASTs were distributed uniformly both in color and magnitude over the CMD and spatially throughout the Magellan/FourStar footprint. We inserted only 5% of the total stars per image to avoid effects of self-crowding. An artificial star was only considered recovered if it passed all the photometric quality cuts applied to the photometry. More details on the photometric quality cuts are available in A. J. Lee et al. (2021).

We adopted a WLM distance modulus of  $\mu_0 = 24.93$  mag (968 kpc). This is the same value used by C25. This choice provides for self-consistency in SFH comparisons. This distance was derived from the tip of the red giant branch (TRGB; S. M. Albers et al. 2019), and is consistent with commonly adopted distances to WLM measured with the TRGB, J-region asymptotic giant branch (JAGB) method, and Cepheids (e.g., A. W.

McConnachie et al. 2005; B. A. Jacobs et al. 2009; A. J. Lee et al. 2021; G. S. Anand et al. 2021).

We adopted a Galactic extinction value of  $A_V = 0.12$  mag from E. F. Schlafly & D. P. Finkbeiner (2011). For a J. A. Cardelli et al. (1989) extinction law and an  $R_V = 3.1$ , this corresponds to  $A_J = 0.03$  mag and  $A_K = 0.01$  mag. We applied these corrections directly to our photometry before modeling the CMD. We did not solve for extinction as part of the CMD modeling. We did not include reddening internal to WLM in our modeling as several studies have already demonstrated that WLM has no measurable internal dust (e.g., S. M. Albers et al. 2019; A. J. Lee et al. 2021; K. B. W. McQuinn et al. 2024b; R. E. Cohen et al. 2025).

We converted the CMD to a Hess diagram with bin sizes of  $0.05 \times 0.05$  mag in color and magnitude, respectively. We then fit the binned CMD down to the 90% completeness limit of  $J = 20.0$  mag. Our fits also included a CMD model of Galactic foreground stars generated from the TRILEGAL simulation (L. Girardi et al. 2005). To accurately account for spatially-dependent observational biases and completeness, we measured the SFH of the inner region of WLM ( $r < r_h$ ) and outer region of WLM ( $r > r_h$ ) separately, and then combined their results to determine the total SFH. In total, 825 stars were used for the SFH fits in the inner and outer regions combined, including TP-AGB, E-AGB, RGB, and RHeB stars.

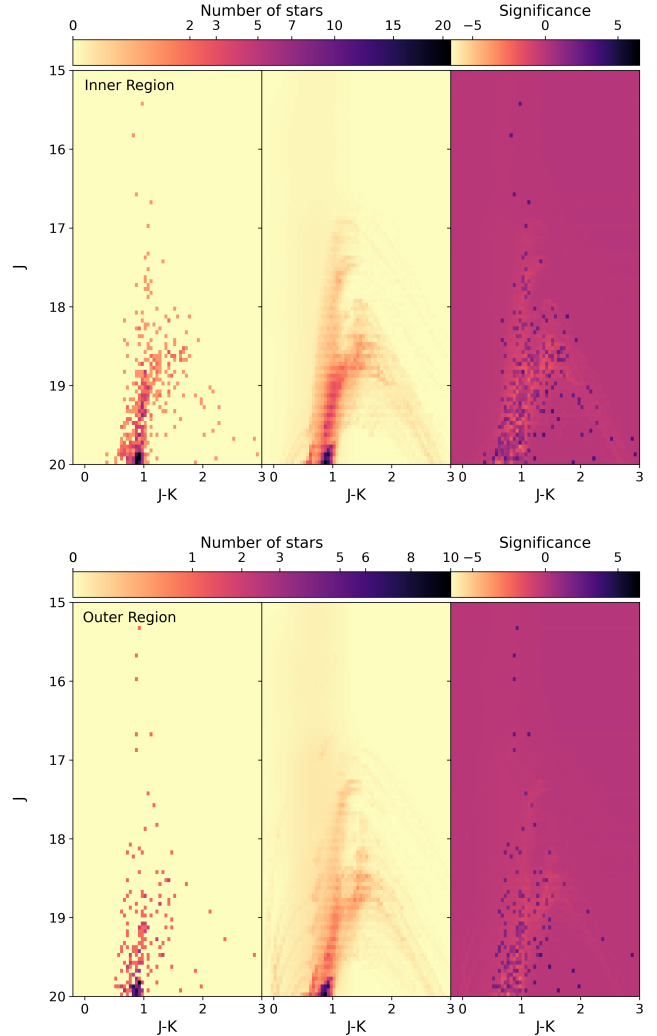
Results of the CMD fits for the inner and outer regions are shown in Figure 4. There is good overall agreement between the observed and model CMDs in both cases. The residual significance plots (right panels) show no notable systematic structures and there appear to be no areas of either the inner or outer CMDs that are poorly modeled.

We calculated random uncertainties using the hybrid Monte Carlo process described in A. E. Dolphin (2013). As discussed in L25, systematic uncertainties for SFHs measured with MATCH are usually computed following the procedure outlined in A. E. Dolphin (2013). However, because there are no other sufficiently realistic AGB star models available, we were unable to adopt this approach and we only consider random uncertainties in this paper.

#### 4. THE STAR FORMATION HISTORY OF WLM

##### 4.1. The Global SFH of WLM from AGB Stars

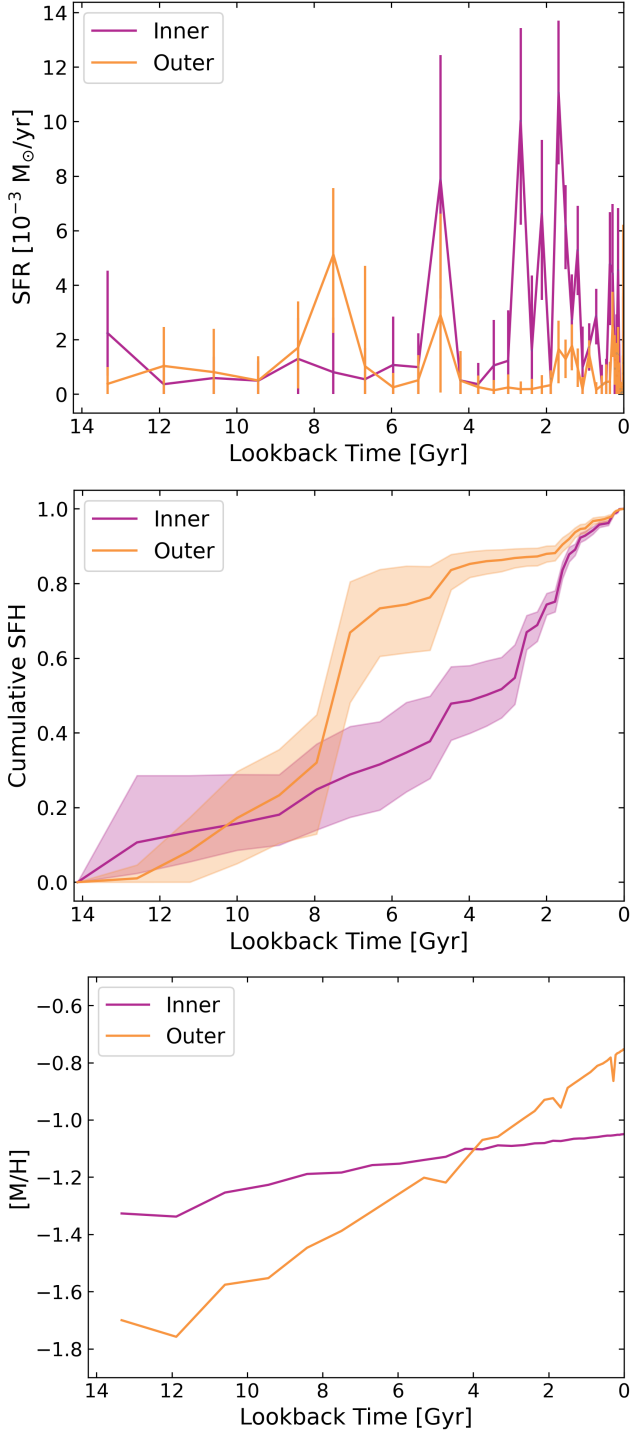
The star formation rates, cumulative star formation history, and age-metallicity relation for the outer and inner regions are shown in Figure 5. The plotted random uncertainties correspond to the 68% confidence interval. We list measured values of  $\tau_{50}$  and  $\tau_{90}$  and their uncertainties for the inner region, outer region, and combined



**Figure 4.** Hess diagrams for our AGB star SFH fits for the observed data (left panel), best-fit linear combination of SSPs (middle panel), and residual CMDs (right panel) for the inner region ( $r < r_h$ , top) and outer region ( $r > r_h$ , bottom). The residuals are expressed in Poisson standard deviations.

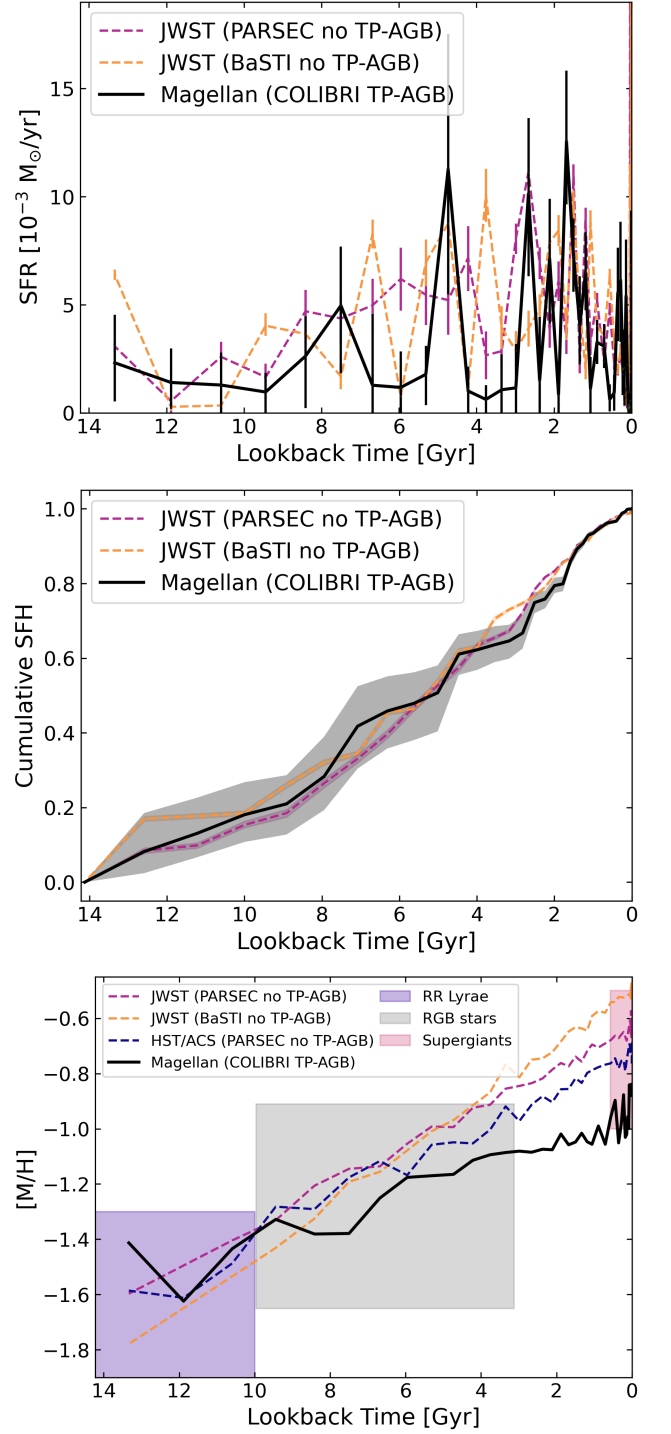
result in Table 1. We discuss further the age gradient in WLM in §6. We note the outer region shows a burst of star formation  $\sim 8$  Gyr ago, not seen in the inner region. We further discuss the potential origin of this burst in §5.

Figure 6 presents the best-fit global cumulative AGB star SFH, SFR as a function of time, and the AMR (thick black line), for the inner and outer regions combined. From the cumulative SFH, we see that WLM had low level SF until a burst  $\sim 8$  Gyr ago, followed by larger bursts  $\sim 5, 3$ , and  $1.5$  Gyr ago. We recovered a total stellar mass in the full FOV of  $M_* = 3.9 \pm 0.3 \times 10^7 M_\odot$ . We converted this to a present-day mass by correcting



**Figure 5.** SFR as a function of time (top), cumulative SFH (middle), and AMR (bottom) derived from the AGB stars for the inner ( $r < r_h$ ) and outer regions ( $r > r_h$ ) of WLM.

for stellar evolution mass loss, which [C. Conroy et al. \(2009\)](#) estimated to be  $\sim 30\%$  for star-forming galaxies. This calculation results in a present-day mass of  $M_{*,z=0} = 2.7 \times 10^7 M_{\odot}$ . This value agrees well with the



**Figure 6.** Top panel: SFR as a function of time. Middle panel: global cumulative SFH. Bottom panel: AMR derived from the AGB stars compared with the oMSTO SFHs. Spectroscopically determined metallicity ranges from RR Lyrae ([A. Sarajedini 2023](#)), RGB stars ([R. Leaman et al. 2009](#)), and supergiants ([M. A. Urbaneja et al. 2008](#)) are shown for reference. Age ranges for the spectroscopic measurements are taken from each of the indicated papers. The magenta and orange lines represent fits derived from the oMSTO using the PARSEC and BaSTI models, respectively, from JWST NIRCcam and NIRISS imaging analyzed in [C25](#), that have been scaled to match the FOV of our ground-based observations. The indigo line represents the fit derived from the oMSTO using the PARSEC models from HST/ACS imaging analyzed in [C25](#).

**Table 1.** Values of  $\tau_{50}$  and  $\tau_{90}$  Obtained from the AGB star SFH and oMSTO fits

| Model                    | $\tau_{50}$ (Gyr)      | $\tau_{90}$ (Gyr)      |
|--------------------------|------------------------|------------------------|
| AGB (Global)             | $5.16^{+2.07}_{-0.50}$ | $1.33^{+0.11}_{-0.09}$ |
| PARSEC                   | $5.29^{+0.34}_{-0.28}$ | $1.42^{+0.16}_{-0.01}$ |
| BaSTI                    | $5.32^{+0.31}_{-0.30}$ | $1.38^{+0.04}_{-0.12}$ |
| AGB (Inner)              | $3.58^{+1.42}_{-0.81}$ | $1.22^{+0.14}_{-0.09}$ |
| PARSEC NIRCcam           | $4.87^{+0.14}_{-0.40}$ | $1.25^{+0.01}_{-0.12}$ |
| BaSTI NIRCcam            | $4.99^{+0.06}_{-0.52}$ | $1.24^{+0.02}_{-0.12}$ |
| AGB (Outer w/ region A)  | $7.48^{+0.46}_{-0.53}$ | $1.62^{+0.40}_{-0.19}$ |
| AGB (Outer w/o region A) | $7.91^{+1.65}_{-1.12}$ | $1.70^{+2.31}_{-0.12}$ |
| PARSEC NIRISS            | $7.76^{+0.31}_{-0.68}$ | $2.90^{+0.27}_{-0.09}$ |
| BaSTI NIRISS             | $8.87^{+0.23}_{-0.92}$ | $3.11^{+0.20}_{-0.29}$ |

**References**—PARSEC and BaSTI values are from R. E. Cohen et al. (2025).

stellar mass of WLM of  $2.8 \times 10^7 M_{\odot}$  calculated from WLM’s 3.6  $\mu\text{m}$  luminosity in D. O. Cook et al. 2014, which we standardized with the same distance modulus used in this study.

The AMR in Figure 6 shows the overall metallicity evolution. The early populations of WLM were metal-poor at  $[M/H] \approx -1.5$  dex. When WLM had formed 50% of its mass, the galaxy had enriched to a metallicity of  $[M/H] \approx -1.2$  dex. Finally, we found the present-day global metallicity of WLM to be  $[M/H] \approx -0.9$  dex. We compare these values to metallicity estimates from the literature in §4.2.

#### 4.2. Comparison to the JWST-based SFH

We now consider how the AGB star SFH compares to the SFH of WLM derived from the oldest MSTO. To validate our results against the SFH measured from the oMSTO in C25, we first needed to scale their SFR to match the stellar mass covered in our FOV. As shown in Figure 1, the C25 SFH is based on a NIRCcam field which covers a portion of WLM’s disk and a NIRISS field which lies  $\sim 1.5$  kpc to the southeast of WLM’s central region.

For the purposes of this exercise, we adopted the NIRCcam-based SFH as the SFH for all area within  $\lesssim 1r_h$  and multiplied it by a factor of  $\sim 3.1$  (i.e., the angular area of  $1r_h$  divided by the angular area of the NIRCcam FOV). Similarly, we assumed that the star formation of the NIRISS field represents the star formation outside of  $1r_h$  and multiplied it by  $\sim 30.1$ . These are clearly approximations, particularly given some of the azimuthal and radial gradients reported by C25. How-

ever, these assumptions are unlikely to introduce large biases in our SFH comparisons. Spatially-matched data that include AGB stars and the oldest MSTO would be ideal (e.g., with Roman), but as discussed in §1, such datasets are currently not available.

In addition to the results from the AGB star SFH as discussed in §4.1, Figure 6 also shows the best-fit results based on the oMSTO from C25 derived from both the BaSTI (S. L. Hidalgo et al. 2018) and PARSEC (A. Bressan et al. 2012) stellar evolution libraries. We plot the 68% random uncertainties reported by C25. The C25 SFHs and uncertainties have been scaled up by the areal coverage factors.

The AGB star SFH and oMSTO SFHs from both the PARSEC and BaSTI models are in excellent agreement. Like the oMSTO-derived SFH, the AGB star SFH recovers that WLM formed 20% of its stellar mass within the first  $\sim 4$  Gyr of its history, and then  $\sim 50\%$  of its stellar mass within the last  $\sim 5$  Gyr. There are minor differences from  $\sim 2 - 4$  Gyr ago, though this is the only time at which the SFHs disagree beyond the 68% uncertainties on the AGB star SFHs. We do not undertake a detailed comparison of recent star formation, as our approach to extrapolating the JWST fields will be far less accurate for younger populations that are not well-mixed. Importantly, the AGB star SFH is well within the model-to-model variations from oMSTO CMD analysis, which is what C25 use to gauge systematic uncertainties in the oldest MSTO SFHs.

In terms of SFH summary statistics (see Table 1), all three fits (oldest MSTO using BaSTI and PARSEC, AGB star) yield consistent values of  $\tau_{50} \approx 5.2 - 5.3$  Gyr ago and  $\tau_{90} \approx 1.3 - 1.4$  Gyr ago. Uncertainties on the AGB star-based values are larger for  $\tau_{50}$  than those from the oldest MSTO. This is likely the result of shot noise and perhaps some age-metallicity degeneracy effects as only 825 stars are being used to measure the AGB star SFH. Uncertainties on  $\tau_{90}$  are comparable between all three SFHs.

All three AMRs show the same qualitative trends (i.e., steady enrichment as a function of linear look-back time), though with modest offsets from one another. Compared to the AGB star based metallicity, the oldest MSTO-based AMRs are slightly more metal-poor at the very oldest ages and show steeper enrichment. To place all three AMRs into context, we overplot several external stellar metallicity estimates for WLM. At ancient times, we include metallicities derived from the periods of 90 RR Lyrae variables, which ranged from  $-2.4 \lesssim [M/H] \lesssim -1.3$  with a mean metallicity of  $[\text{Fe}/\text{H}] = -1.74$  (A. Sarajedini 2023). We assume RR Lyrae corresponds to stars older than  $\sim 10$  Gyr.

For intermediate ages, we include RGB star metallicities derived from spectroscopy of WLM red giants from R. Leaman et al. (2009), who derived a mean metallicity of  $[\text{Fe}/\text{H}] = -1.28$  ( $\sigma = 0.37$ ). We plot these over the age range provided in the R. Leaman et al. (2009) paper. Finally, we include present day stellar metallicity estimates from M. A. Urbaneja et al. (2008). They derived a stellar metallicity range from six BA-type supergiants of  $-1.0 \lesssim [\text{M}/\text{H}] \lesssim -0.5$  with a mean stellar metallicity of  $[\text{M}/\text{H}] = -0.87$ .

All three CMD-based AMRs are within the ranges reported by these independent metallicity estimates. The modest offsets and slightly different AMRs between the AGB stars and oldest MSTO methods are interesting, but without more suitable datasets it is challenging to explore the causes of any differences (e.g., *does the small number of stars play a role? How does dredge up affect AGB star metallicities?*). For the present purposes, the AMRs from the three approaches are in good agreement, and certainly are comparable to, or better than, AMRs measured historically from different CMD fitting codes (e.g., E. D. Skillman & C. Gallart 2002). We also include the AMR derived from the oMSTO using the PARSEC model from HST/ACS imaging analyzed in C25 as an additional comparison point, demonstrating differences between the AMRs derived from HST and JWST are comparable to differences between the AMRs derived from HST and the AGB stars.

### 5. AN ACCRETION EVENT IN WLM'S NORTHWESTERN OUTER DISK?

While inspecting the SFHs of the inner and outer fields shown in Figure 5, we noticed a burst of star formation at intermediate ages ( $\sim 8$  Gyr) recovered only in the outer field. This burst was not seen in the outer fields of the C25 analysis, who analyzed HST WFC3/UVIS and JWST NIRISS fields in the southeast and western outer regions of WLM, both at  $R \approx 2.5r_h$ . Nor was it observed in the central HST/ACS field analyzed by S. M. Albers et al. (2019).

By examining the CMD and spatial distribution of stars from our NIR data, we found that this burst appears to be due to an over-density of 49 AGB stars located in the northwestern outer disk of WLM, which we label region ‘A’ in Figure 3. It is visible in optical images, such as in Figure 1 (see also D. C. Jackson et al. 2007). Region A also spatially coincides with a known warp in H I observations (e.g., D. C. Jackson et al. 2004; E. W. Koch et al. 2025), as shown in Figure 7. We note this over-density is distinct from WLM’s only known globular cluster, WLM-1, which is located on the western edge of WLM’s outer disk (H. D. Ables & P. G. Ables

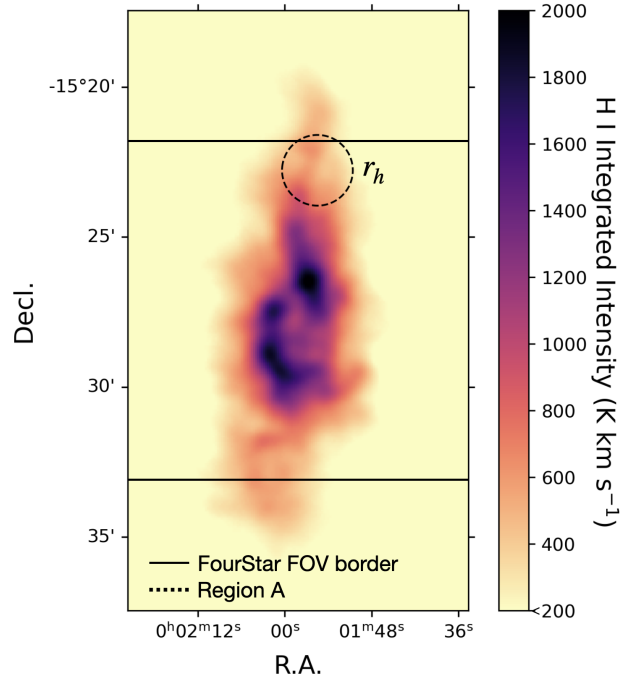


**Figure 7.** H I integrated intensity map from E. W. Koch et al. (2025) overlaid with the Magellan/FourStar footprint (solid lines). The half-light circle of Region ‘A’ is denoted by the dotted line.

1977; A. Sandage & G. Carlson 1985; P. W. Hodge et al. 1999).

To characterize the stellar populations of this over-density, as well as its impact on our global SFH, we re-fit the SFH of the outer region ( $r > r_h$ ) with region A excluded. We show the resulting fit in Figure 8. The burst at 8 Gyr seen in Figure 6 disappears. Then, to fit the SFH of just region A, we first removed the contribution of the outer region’s intrinsic SF, by adding the outer region’s CMD as a ‘background CMD’ to Region A’s MATCH parameter file, scaled down by a factor of  $\sim 0.05$  (i.e., the angular area of the outer region divided by the angular area of region A). The resulting SFH fit for region A only is shown in the top panel of Figure 9. The uncertainties are large, as expected, because the SFH is based on only 49 stars. Qualitatively, there appears to be little-to-modest ancient star formation in this region with a rapid increase at  $\sim 8$  Gyr ago. This was followed by another period of roughly constant star formation. We calculated the total stellar mass of region A to be  $M_* = 3.3 \pm 0.8 \times 10^6 M_\odot$  and that it formed 50% of its stellar mass  $\tau_{50} = 7.5^{+1.7}_{-0.9}$  Gyr ago. We model the light profile of the over-density by fitting an exponential light profile (e.g., as described in N. F. Martin et al. 2008, 2016) to the AGB and RGB stars (down to the 80% completeness level of the photome-

try) and find a half-light radius of  $r_h = 338 \pm 167$  pc. The half-light profile is shown as a pink circle in Figure 1.

We speculate on possible origins for this over-density of intermediate-age stars. First, we consider the possibility that region A is a star cluster that formed *in situ* in WLM, possibly due to its location near the end of a reported bar in WLM (N. Kolhe et al. 2026). This seems unlikely as region A’s radius of 338 pc is significantly larger than the radii of even the most massive star clusters, which have half-light radii of  $\sim 100$  pc (e.g., M. R. Krumholz et al. 2019). Given its large stellar mass and older age, it also seems unlikely to be a massive  $\sim 8$  Gyr cluster that is still in the process of dissolving, as most massive clusters dissolve on timescales of  $\lesssim 1$  Gyr (e.g., E. Bica et al. 2001; S. F. Portegies Zwart et al. 2001, 2010; J. M. D. Kruijssen et al. 2011).

A second possibility is that this over-density is an accreted satellite galaxy. WLM has long been considered an archetypal ‘isolated’ dwarf galaxy, and therefore an ideal testbed for understanding how low-mass galaxies evolve when unperturbed from external environmental effects, such as ram pressure or tidal effects (e.g., R. Leaman et al. 2009; S. M. Albers et al. 2019; A. Sarajedini 2023; H. N. Archer et al. 2024; K. B. W. McQuinn et al. 2024b; R. E. Cohen et al. 2025). However, several pieces of evidence suggest WLM has actually had a recent interaction. The first is the aforementioned spatial association of an H I warp with this stellar over-density; simulations by M. Khademi et al. (2021) have shown this warp may have been caused by a minor merger in WLM’s past. Second, K. A. Venn et al. (2003) found nebular oxygen abundances derived from H II regions in WLM were  $\sim 5\times$  lower than stellar oxygen abundances derived from its A-type supergiants (see also H. Lee et al. 2005). K. A. Venn et al. (2003) suggested one plausible explanation for this discrepancy was that a massive ( $> 10^6 M_\odot$ ) H I cloud merged and rapidly mixed with WLM’s ISM in the past  $\sim 10$  Myr (i.e., the age of A-type supergiants), thus diluting WLM’s H II regions.

Third, is region A’s similarity to other well-studied dwarf galaxies. We compare region A’s properties to other globular clusters and dwarf galaxies in the Local Volume, whose present-day masses (calculated from their  $M_V$  values using a mass-to-light ratio of 2) and sizes have been compiled in A. B. Pace (2025). First, we convert region A’s CMD-based total stellar mass to a present-day stellar mass by accounting for stellar evolution mass loss effects, which C. Conroy et al. (2009) estimates to be  $\sim 40\%$  for older, faint galaxies. Applying this correction to our total stellar mass yields a

present-day mass of  $M_{*,z=0} \approx 2.0 \times 10^6 M_\odot$ . In Figure 9, we plot region A on the luminosity-size relation for globular clusters and dwarf galaxies in the Local Volume compiled in A. B. Pace (2025). Furthermore, in Figure 9, we compare the cumulative SFH of region A to the SFHs of Pegasus and Leo II (A. Savino et al. 2025; D. R. Weisz et al. 2014b), two dwarf galaxies with similar masses and sizes to region A. Both these comparisons demonstrate region A’s mass, size, and SFH are broadly similar to other dwarf galaxies in the Local Volume.

In one scenario, region A could have been accreted  $\sim 8$  Gyr ago, triggering the burst of star formation in that area. Or, it could have been a dwarf galaxy accreted more recently, which could explain the peculiar abundance patterns found in K. A. Venn et al. (2003) and region A’s spatial association with H I disturbance in that area of WLM (D. C. Jackson et al. 2004; E. W. Koch et al. 2025). Further data, such as an oldest MSTO-based SFH which would decrease the SFH uncertainties and spectroscopic observations (e.g., kinematics, metallicities), would deliver a clearer picture of region A’s origin.

More broadly, the discovery of this over-density, regardless of its origin, is another demonstration for discovery and characterization potential of wide-area, NIR imaging of AGB stars in nearby galaxies.

## 6. POPULATION GRADIENTS IN WLM

### 6.1. WLM’s Age Gradient

Comparing the SFHs of the inner ( $r < r_h$ ) and outer ( $r > r_h$ , excluding region A) regions in Figure 8 reveals a clear age gradient in WLM. We find the inner region formed 50% of its stellar mass  $\sim 3.6$  Gyr ago, making it a fairly young region, whereas the outer region (without region A) formed 50% of its stellar mass  $\sim 7.9$  Gyr ago, making it older on average. This age gradient is consistent with the ‘outside-in’ radial stellar age gradient observed in most dwarf galaxies, where the stellar populations in the outskirts are on average older than in the central regions (e.g., R. C. Dohm-Palmer et al. 1998; J. S. Gallagher et al. 1998; M. G. Lee et al. 1999; A. Aparicio et al. 2000; J. T. A. de Jong et al. 2008; A. del Pino et al. 2013; S. L. Hidalgo et al. 2013; K. B. W. McQuinn et al. 2017; A. Savino et al. 2019). These age gradients are a result of stellar feedback, which drives stars initially formed in the central regions to the outskirts (e.g., K. El-Badry et al. 2016; M. L. M. Collins & J. I. Read 2022).

We note we also find good agreement in the qualitative shapes of our inner and outer SFHs with the C25 NIRCcam-based SFH and NIRISS-based SFH shown in Figure 8, where we assumed that the star formation of

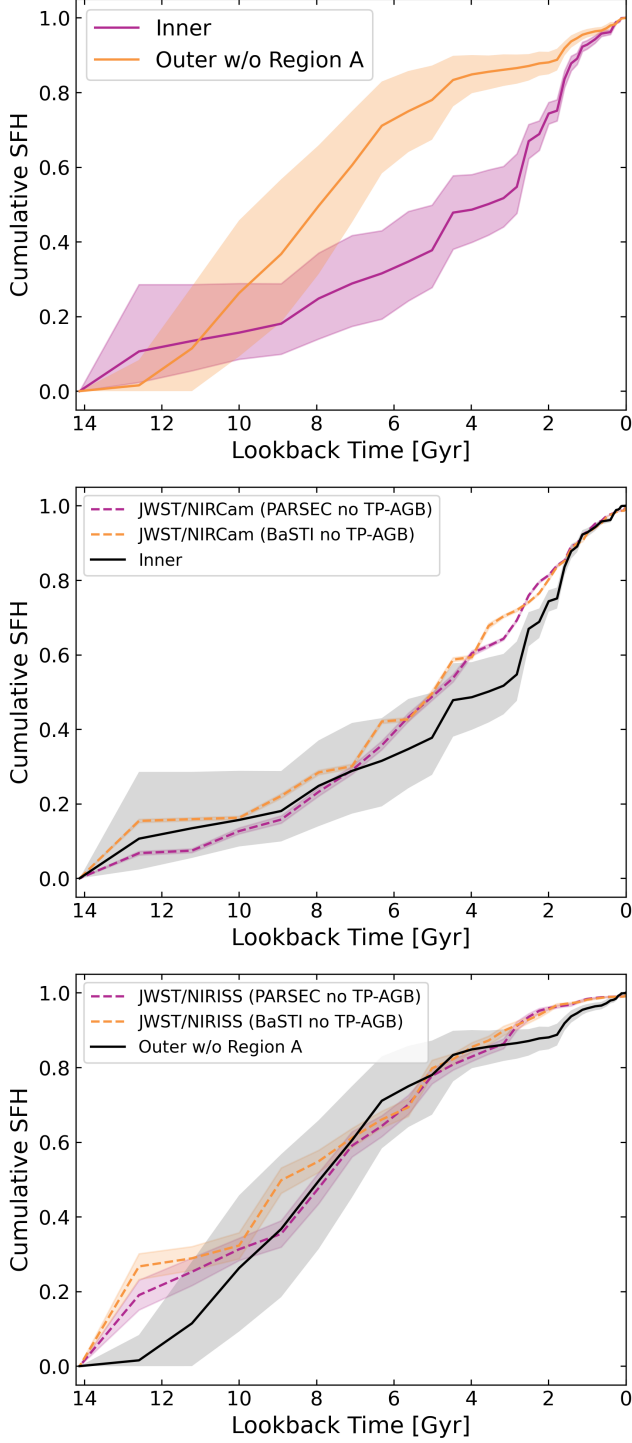


**Figure 8.** Top panel: cumulative star formation history for the inner ( $r < r_h$ ) outer region ( $r > r_h$ ) excluding region A. Middle panel: cumulative star formation history for the inner region. The magenta and orange lines represent fits derived from the oMSTO using the PARSEC and BaSTI models, respectively, for the C25 JWST/NIRCam field. Bottom panel: cumulative star formation history for the outer region ( $r > r_h$ ), excluding region A. The magenta and orange lines represent fits derived from the oMSTO using the PARSEC and BaSTI models, respectively, for the C25 JWST/NIRISS field.

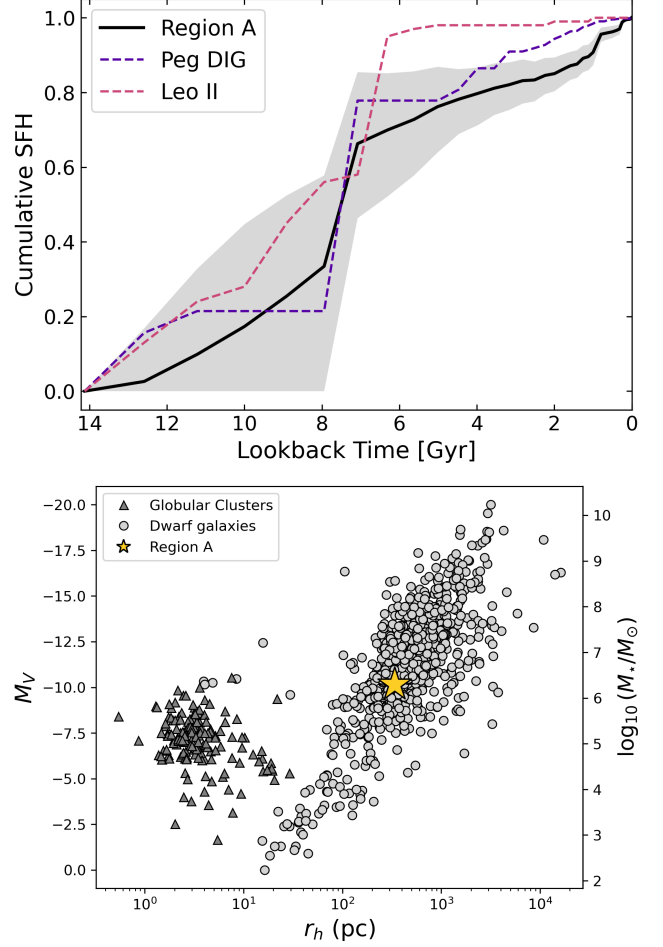


**Figure 9.** Top panel: Cumulative star formation history for region A only. The spatial extent of region A is shown in Figure 3. Overplotted are SFHs for Pegasus and Leo II, two dwarf galaxies with similar masses and sizes to region A (A. Savino et al. 2025; D. R. Weisz et al. 2014b). Bottom panel: Luminosity-size relationship for globular clusters and dwarf galaxies in the Local Volume (LV). Region A is denoted with a gold star. This figure has been modified from Figure 8 of A. B. Pace (2025), who computed the masses assuming a mass-to-light ratio of 2.

the NIRCcam and NIRISS fields represent the star formation inside and outside of  $1 r_h$ , respectively. We also find good statistical agreement with C25 in our measured values of  $\tau_{90}$  and  $\tau_{50}$  in the inner and outer regions, which are listed in Table 1.

## 6.2. WLM's Metallicity Gradient

While our study and others have found WLM has a steep age gradient (e.g., S. M. Albers et al. 2019; R. E. Cohen et al. 2025), R. Leaman et al. (2013) found WLM has a weak metallicity gradient of  $-0.04$  dex  $\text{kpc}^{-1}$  out to  $\sim 2r_h$  on the major axis. Simulations have shown that galaxies with weaker metallicity gradients tend to

be younger on average, because recent, metal-rich star formation washes out pre-existing metallicity gradients caused by the radial migration of older, metal-poor stars (K. El-Badry et al. 2016; F. J. Mercado et al. 2021). This picture is consistent with our measured value of  $\tau_{50} \approx 5.2$  Gyr, which suggests WLM is a relatively young galaxy compared with other LG dwarf galaxies (e.g., D. R. Weisz et al. 2014b), and is thus expected to have a weak metallicity gradient (e.g., S. Taibi et al. 2022; S. W. Fu et al. 2024).

## 7. FUTURE PROSPECTS

AGB star SFHs are well-suited for NIR observations with facilities such as Roman, Euclid, and JWST. Roman and Euclid can resolve AGB stars in the outer disks and halos of galaxies out to  $\sim 10$  Mpc. JWST can resolve AGB stars in the inner disks of galaxies out to  $\sim 10$  Mpc, and in the outer disks and halos of galaxies out to tens of Mpc. Because they are significantly brighter than other features (e.g., AGB stars are  $\sim 100\times$  brighter than RC stars) similar SFH science can be achieved with AGB stars for less integration time.

We illustrate the observational efficiency of AGB star SFHs by comparing hypothetical JWST observations of AGB stars and RC stars as a function of galaxy distance using the JWST exposure time calculator (ETC)<sup>4</sup> (A. Savino et al. 2024). These exposure times are listed in Table 2. We do not include crowding in this exercise, though note that it is far more likely to affect RC stars than AGB stars.

To simulate the observational time needed for the AGB star SFHs, we calculated the exposure time needed to resolve stars 1 mag below the TRGB at an SNR = 5 in the F115W filter in NIRCams SW channel (pixel scale:  $0.031''$  pixel<sup>-1</sup>) and at a SNR of SNR  $\approx 7$  in the F277W filter in the LW channel (pixel scale:  $0.063''$  pixel<sup>-1</sup>). Measuring the color comes at no additional cost for JWST, which can observe simultaneously with the SW and LW channels. Even the LW channel on JWST is sufficiently sharp to resolve AGB stars at  $\gtrsim 40$  Mpc (e.g., S. Li et al. 2025). Our limited testing suggests this is the most efficient color combination for AGB star SFH measurements. These SNR requirements  $\sim 1$  mag below the TRGB are standard for datasets used to measure precise TRGB and JAGB distances with JWST (e.g., M. J. B. Newman et al. 2024; W. L. Freedman et al. 2025), which are well-matched for also measuring AGB star SFHs.

For RC SFHs, we adopt the filters F115W and F200W and assume that observations need to extend  $\sim 1$  mag below the RC. The faintness of the RC increases the

effects of crowding, making it necessary to use two SW filters, as opposed to one SW and one LW filter. This particular filter combination has been prevalent in the JWST-based CMDs that target the RC (e.g., N. Habel et al. 2024; C. Nally et al. 2024; G. Bortolini et al. 2025; A. Ck et al. 2025; M. Correnti et al. 2025). The need to reach  $\sim 1$  mag below the RC is motivated by the need to minimize systematics on the SFHs, which can become quite large if entire RC is not included on the CMD (e.g., A. E. Dolphin 2012; D. R. Weisz et al. 2014b). Accordingly, we calculated the exposure time needed to resolve stars 1 mag below the median RC magnitude in the F115W filter at a color of  $F115W - F200W < 1$  (i.e., the blue edge of the RC) at an SNR = 5.

The results of this exercise are summarized in Table 2. They demonstrate that AGB star SFHs are  $100\times$  more observationally efficient than RC-based SFHs, even without factoring in crowding effects. At  $D \sim 7$  Mpc, it only takes JWST 4 min to reach our target depth for AGB stars compared to 8 hours for the RC. The difference is more pronounced at  $D \sim 13$  Mpc. Beyond this distance, effectively the edge of the Local Volume, JWST requires prohibitively long integration times to resolve the entire RC.

This analysis is supported by JWST observations in the literature. AGB stars have been resolved with NIRCams in the Virgo cluster ( $d = 16$  Mpc) in 18 min (e.g., G. S. Anand et al. 2025), in disk galaxies at  $D \sim 21$  Mpc in 48 min (e.g., W. L. Freedman et al. 2025). Brighter AGB stars ( $M_J \lesssim -5$ ) have already been resolved in a galaxy at a distance of  $d = 40$  Mpc with JWST in 2 hours of exposure time (S. Li et al. 2025). Scaling from crowding and sensitivity estimates from these datasets, it is likely that JWST can resolve AGB stars in the halos of galaxies out to  $D \gtrsim 50$  Mpc in modest integration times (e.g., tens of hours). Indeed, one ambitious JWST program is even targeting resolved AGB stars in the Coma Cluster ( $D \sim 100$  Mpc) by making use of JWST’s extremely wide-pass filters (JWST-GO-6876, PI: W. Freedman), which, if successful, could extend resolved star-based SFHs to distances that have been previously unimaginable.

## 8. CONCLUSION

Using NIR observations of resolved AGB stars, we derived the lifetime SFH of the Local Group galaxy WLM. We find that the SFH measured from AGB stars is in excellent agreement with the SFH measured from a deep CMD at the depth of the oMSTO. We also recover an age gradient in good agreement with the age gradient measured from deep JWST data, where we find the outer

<sup>4</sup> <https://jwst.etc.stsci.edu/>

**Table 2.** JWST/NIRCam exposure times required to resolve stellar populations at a SNR = 5

| Distance (Mpc) | Total AGB <sup>a</sup> | RC magnitude <sup>b</sup> | RC color <sup>c</sup> | Total RC |
|----------------|------------------------|---------------------------|-----------------------|----------|
| 7              | 4 min                  | 4 hr                      | 4 hr                  | 8 hr     |
| 13             | 12 min                 | 79 hr                     | 70 hr                 | 149 hr   |
| 21             | 48 min                 | ...                       | ...                   | ...      |
| 40             | 5 hr                   | ...                       | ...                   | ...      |

<sup>a</sup>1 mag below TRGB<sup>b</sup>1 mag below median RC magnitude<sup>c</sup> $F115W - F200W < 1$ 

regions of WLM are older on average than the younger regions.

This test demonstrates that AGB stars can produce lifetime SFHs comparable in fidelity and detail to those currently available in and around the Local Group, albeit with the potential to do so in galaxies at distances out to  $\sim 50$  Mpc. Several ongoing efforts to improve AGB star models and age calibrations (e.g., [M. L. Boyer et al. 2013](#); [K. Huynh et al. 2025](#)) and JWST-GO-6852, PI: S. Goldman) will continue to make AGB star SFHs even more powerful.

We also identified an over-density of AGB stars in the northwestern outer disk of WLM, associated with a burst of star formation  $\sim 8$  Gyr ago. We speculate is likely an accreted satellite galaxy, given its size and inferred stellar mass ( $r_h = 338$  pc,  $M_* = 2.0 \times 10^6 M_\odot$ ). Our characterization of this system is coarse as only  $\sim 50$  AGB stars are associated with it. A more precise SFH derived from a well-populated CMD at the depth of the oMSTO would significantly improve our understanding of this unusual feature. Beyond revealing the intriguing hints of a low-mass past accretion event, this finding demonstrates the power of wide-field NIR imaging for the efficient discovery and characterization of substructure in galaxies.

## ACKNOWLEDGMENTS

We thank Roger Cohen for graciously supplying us with his star formation history fits. We also acknowledge Wendy Freedman, Barry Madore, and Andy Monson for their observing contributions.

AJL is supported by NASA through the NASA Hubble Fellowship grant #HST-HF2-51580.001 awarded by the Space Telescope Science Institute, which is operated by the Association of Universities for Research in Astronomy, Inc., for NASA, under contract NAS5-26555.

This research has made use of NASA’s Astrophysics Data System Bibliographic Services. This research has made use of the NASA/IPAC infrared Science Archive (IRSA), which is operated by the Jet Propulsion Laboratory, California Institute of Technology, under contract with the National Aeronautics and Space Administration. This paper includes data gathered with the 6.5 meter Magellan Telescopes located at Las Campanas Observatory, Chile. This paper uses data from the Local Group L-Band survey (LGLBS), which is an Extra Large program conducted on Jansky Very Large Array, and is operated by the National Radio Astronomy Observatory (NRAO) and includes observations from VLA projects 20A-346, 13A-213, 14A-235, 14B-088, 14B-212, 15A-175, 17B-162, and GBT projects 09A-017, 13A-420, 13A-430, 13B-169, 14A-367, 16A-413. NRAO is a facility of the National Science Foundation operated under cooperative agreement by Associated Universities, Inc. Execution of the LGLBS survey science was supported by NSF Award 2205628.

*Facilities:* Magellan/FourStar

*Software:* Astropy ([Astropy Collaboration et al. 2013, 2018, 2022](#)), DAOPHOT ([P. B. Stetson 1987, 1994, 2011](#)), `imf` (<https://github.com/keflavich/imf>), MATCH ([A. E. Dolphin 2002, 2012, 2013, 2016](#)), Matplotlib ([J. D. Hunter 2007](#)), NumPy ([C. R. Harris et al. 2020](#)), Pandas ([W. McKinney 2010](#)), Scikit-learn ([F. Pedregosa et al. 2011](#))

## REFERENCES

Ables, H. D., & Ables, P. G. 1977, *ApJS*, 34, 245, doi: [10.1086/190449](https://doi.org/10.1086/190449)

Albers, S. M., Weisz, D. R., Cole, A. A., et al. 2019, *MNRAS*, 490, 5538, doi: [10.1093/mnras/stz2903](https://doi.org/10.1093/mnras/stz2903)

- Anand, G. S., Rizzi, L., Tully, R. B., et al. 2021, *AJ*, 162, 80, doi: [10.3847/1538-3881/ac0440](https://doi.org/10.3847/1538-3881/ac0440)
- Anand, G. S., Tully, R. B., Cohen, Y., et al. 2025, *ApJ*, 982, 26, doi: [10.3847/1538-4357/adb399](https://doi.org/10.3847/1538-4357/adb399)
- Aparicio, A., Tikhonov, N., & Karachentsev, I. 2000, *AJ*, 119, 177, doi: [10.1086/301157](https://doi.org/10.1086/301157)
- Archer, H. N., Hunter, D. A., Elmegreen, B. G., et al. 2024, *AJ*, 167, 274, doi: [10.3847/1538-3881/ad3f18](https://doi.org/10.3847/1538-3881/ad3f18)
- Astropy Collaboration, Robitaille, T. P., Tollerud, E. J., et al. 2013, *A&A*, 558, A33, doi: [10.1051/0004-6361/201322068](https://doi.org/10.1051/0004-6361/201322068)
- Astropy Collaboration, Price-Whelan, A. M., Sipőcz, B. M., et al. 2018, *AJ*, 156, 123, doi: [10.3847/1538-3881/aabc4f](https://doi.org/10.3847/1538-3881/aabc4f)
- Astropy Collaboration, Price-Whelan, A. M., Lim, P. L., et al. 2022, *ApJ*, 935, 167, doi: [10.3847/1538-4357/ac7c74](https://doi.org/10.3847/1538-4357/ac7c74)
- Bastian, N., Weisz, D. R., Skillman, E. D., et al. 2011, *MNRAS*, 412, 1539, doi: [10.1111/j.1365-2966.2010.17841.x](https://doi.org/10.1111/j.1365-2966.2010.17841.x)
- Bernard, E. J., Ferguson, A. M. N., Richardson, J. C., et al. 2015, *MNRAS*, 446, 2789, doi: [10.1093/mnras/stu2309](https://doi.org/10.1093/mnras/stu2309)
- Bica, E., Santiago, B. X., Dutra, C. M., et al. 2001, *A&A*, 366, 827, doi: [10.1051/0004-6361:20000248](https://doi.org/10.1051/0004-6361:20000248)
- Bortolini, G., Correnti, M., Adamo, A., et al. 2025, *ApJ*, 991, 212, doi: [10.3847/1538-4357/adfccc](https://doi.org/10.3847/1538-4357/adfccc)
- Boyer, M. L., Skillman, E. D., van Loon, J. T., Gehrz, R. D., & Woodward, C. E. 2009, *ApJ*, 697, 1993, doi: [10.1088/0004-637X/697/2/1993](https://doi.org/10.1088/0004-637X/697/2/1993)
- Boyer, M. L., Girardi, L., Marigo, P., et al. 2013, *ApJ*, 774, 83, doi: [10.1088/0004-637X/774/1/83](https://doi.org/10.1088/0004-637X/774/1/83)
- Boyer, M. L., Williams, B. F., Aringer, B., et al. 2019, *ApJ*, 879, 109, doi: [10.3847/1538-4357/ab24e2](https://doi.org/10.3847/1538-4357/ab24e2)
- Bressan, A., Marigo, P., Girardi, L., et al. 2012, *MNRAS*, 427, 127, doi: [10.1111/j.1365-2966.2012.21948.x](https://doi.org/10.1111/j.1365-2966.2012.21948.x)
- Brown, T. M., Smith, E., Ferguson, H. C., et al. 2006, *ApJ*, 652, 323, doi: [10.1086/508015](https://doi.org/10.1086/508015)
- Brown, T. M., Tumlinson, J., Geha, M., et al. 2014, *ApJ*, 796, 91, doi: [10.1088/0004-637X/796/2/91](https://doi.org/10.1088/0004-637X/796/2/91)
- Cardelli, J. A., Clayton, G. C., & Mathis, J. S. 1989, *ApJ*, 345, 245, doi: [10.1086/167900](https://doi.org/10.1086/167900)
- Chen, Y., Bressan, A., Girardi, L., et al. 2015, *MNRAS*, 452, 1068, doi: [10.1093/mnras/stv1281](https://doi.org/10.1093/mnras/stv1281)
- Chen, Y., Girardi, L., Bressan, A., et al. 2014, *MNRAS*, 444, 2525, doi: [10.1093/mnras/stu1605](https://doi.org/10.1093/mnras/stu1605)
- Cignoni, M., Sacchi, E., Aloisi, A., et al. 2018, *ApJ*, 856, 62, doi: [10.3847/1538-4357/aab041](https://doi.org/10.3847/1538-4357/aab041)
- Cignoni, M., Sacchi, E., Tosi, M., et al. 2019, *ApJ*, 887, 112, doi: [10.3847/1538-4357/ab53d5](https://doi.org/10.3847/1538-4357/ab53d5)
- Cioni, M.-R. L., Girardi, L., Marigo, P., & Habing, H. J. 2006a, *A&A*, 448, 77, doi: [10.1051/0004-6361:20053933](https://doi.org/10.1051/0004-6361:20053933)
- Cioni, M.-R. L., Girardi, L., Marigo, P., & Habing, H. J. 2006b, *A&A*, 452, 195, doi: [10.1051/0004-6361:20054699](https://doi.org/10.1051/0004-6361:20054699)
- Cioni, M.-R. L., & Habing, H. J. 2003, *A&A*, 402, 133, doi: [10.1051/0004-6361:200302226](https://doi.org/10.1051/0004-6361:200302226)
- Cioni, M.-R. L., & Habing, H. J. 2005, *A&A*, 429, 837, doi: [10.1051/0004-6361:20041608](https://doi.org/10.1051/0004-6361:20041608)
- Cioni, M.-R. L., Irwin, M., Ferguson, A. M. N., et al. 2008, *A&A*, 487, 131, doi: [10.1051/0004-6361:200809366](https://doi.org/10.1051/0004-6361:200809366)
- Ck, A., Mayya, D., Bressan, A., & Alzate Trujillo, J. A. 2025, *ApJ*, 984, 21, doi: [10.3847/1538-4357/adc105](https://doi.org/10.3847/1538-4357/adc105)
- Cohen, R. E., McQuinn, K. B. W., Savino, A., et al. 2025, *ApJ*, 981, 153, doi: [10.3847/1538-4357/adb61d](https://doi.org/10.3847/1538-4357/adb61d)
- Cole, A. A., Weisz, D. R., Dolphin, A. E., et al. 2014, *ApJ*, 795, 54, doi: [10.1088/0004-637X/795/1/54](https://doi.org/10.1088/0004-637X/795/1/54)
- Cole, A. A., Skillman, E. D., Tolstoy, E., et al. 2007, *ApJL*, 659, L17, doi: [10.1086/516711](https://doi.org/10.1086/516711)
- Collins, M. L. M., & Read, J. I. 2022, *Nature Astronomy*, 6, 647, doi: [10.1038/s41550-022-01657-4](https://doi.org/10.1038/s41550-022-01657-4)
- Conroy, C. 2013, *ARA&A*, 51, 393, doi: [10.1146/annurev-astro-082812-141017](https://doi.org/10.1146/annurev-astro-082812-141017)
- Conroy, C., Gunn, J. E., & White, M. 2009, *ApJ*, 699, 486, doi: [10.1088/0004-637X/699/1/486](https://doi.org/10.1088/0004-637X/699/1/486)
- Cook, D. O., Dale, D. A., Johnson, B. D., et al. 2014, *MNRAS*, 445, 899, doi: [10.1093/mnras/stu1787](https://doi.org/10.1093/mnras/stu1787)
- Correnti, M., Bortolini, G., Dell'Agli, F., et al. 2025, *ApJ*, 990, 72, doi: [10.3847/1538-4357/adc74](https://doi.org/10.3847/1538-4357/adc74)
- Costa, E., & Frogel, J. A. 1996, *AJ*, 112, 2607, doi: [10.1086/118206](https://doi.org/10.1086/118206)
- Crnojević, D., Ferguson, A. M. N., Irwin, M. J., et al. 2013, *MNRAS*, 432, 832, doi: [10.1093/mnras/stt494](https://doi.org/10.1093/mnras/stt494)
- Dalcanton, J. J., Williams, B. F., Seth, A. C., et al. 2009, *ApJS*, 183, 67, doi: [10.1088/0067-0049/183/1/67](https://doi.org/10.1088/0067-0049/183/1/67)
- Davidge, T. J. 2003, *ApJ*, 597, 289, doi: [10.1086/378271](https://doi.org/10.1086/378271)
- Davidge, T. J. 2005, *AJ*, 130, 2087, doi: [10.1086/491706](https://doi.org/10.1086/491706)
- Davidge, T. J. 2014, *ApJ*, 791, 66, doi: [10.1088/0004-637X/791/1/66](https://doi.org/10.1088/0004-637X/791/1/66)
- de Boer, T. J. L., Tolstoy, E., Lemasle, B., et al. 2014, *A&A*, 572, A10, doi: [10.1051/0004-6361/201424119](https://doi.org/10.1051/0004-6361/201424119)
- de Boer, T. J. L., Tolstoy, E., Saha, A., et al. 2011, *A&A*, 528, A119, doi: [10.1051/0004-6361/201016398](https://doi.org/10.1051/0004-6361/201016398)
- de Boer, T. J. L., Tolstoy, E., Hill, V., et al. 2012a, *A&A*, 539, A103, doi: [10.1051/0004-6361/201118378](https://doi.org/10.1051/0004-6361/201118378)
- de Boer, T. J. L., Tolstoy, E., Hill, V., et al. 2012b, *A&A*, 544, A73, doi: [10.1051/0004-6361/201219547](https://doi.org/10.1051/0004-6361/201219547)
- de Jong, J. T. A., Harris, J., Coleman, M. G., et al. 2008, *ApJ*, 680, 1112, doi: [10.1086/587835](https://doi.org/10.1086/587835)
- del Pino, A., Hidalgo, S. L., Aparicio, A., et al. 2013, *MNRAS*, 433, 1505, doi: [10.1093/mnras/stt833](https://doi.org/10.1093/mnras/stt833)
- Dohm-Palmer, R. C., Skillman, E. D., Gallagher, J., et al. 1998, *AJ*, 116, 1227, doi: [10.1086/300514](https://doi.org/10.1086/300514)

- Dolphin, A. E. 2002, *MNRAS*, 332, 91,  
doi: [10.1046/j.1365-8711.2002.05271.x](https://doi.org/10.1046/j.1365-8711.2002.05271.x)
- Dolphin, A. E. 2012, *ApJ*, 751, 60,  
doi: [10.1088/0004-637X/751/1/60](https://doi.org/10.1088/0004-637X/751/1/60)
- Dolphin, A. E. 2013, *ApJ*, 775, 76,  
doi: [10.1088/0004-637X/775/1/76](https://doi.org/10.1088/0004-637X/775/1/76)
- Dolphin, A. E. 2016, DOLPHOT: Stellar photometry,,  
Astrophysics Source Code Library, record ascl:1608.013
- Dolphin, A. E., Saha, A., Skillman, E. D., et al. 2003, *AJ*,  
126, 187, doi: [10.1086/375761](https://doi.org/10.1086/375761)
- Durbin, M. J., Choi, Y., Savino, A., et al. 2025, *ApJ*, 992,  
106, doi: [10.3847/1538-4357/ae00c8](https://doi.org/10.3847/1538-4357/ae00c8)
- El-Badry, K., Wetzel, A., Geha, M., et al. 2016, *ApJ*, 820,  
131, doi: [10.3847/0004-637X/820/2/131](https://doi.org/10.3847/0004-637X/820/2/131)
- Freedman, W. L., Madore, B. F., Hoyt, T. J., et al. 2025,  
*ApJ*, 985, 203, doi: [10.3847/1538-4357/adce78](https://doi.org/10.3847/1538-4357/adce78)
- Frogel, J. A., & Blanco, V. M. 1983, *ApJL*, 274, L57,  
doi: [10.1086/184150](https://doi.org/10.1086/184150)
- Fu, S. W., Weisz, D. R., Starkenburg, E., et al. 2024, *ApJ*,  
965, 36, doi: [10.3847/1538-4357/ad25ed](https://doi.org/10.3847/1538-4357/ad25ed)
- Gaia Collaboration, Prusti, T., de Bruijne, J. H. J., et al.  
2016, *A&A*, 595, A1, doi: [10.1051/0004-6361/201629272](https://doi.org/10.1051/0004-6361/201629272)
- Gaia Collaboration, Vallenari, A., Brown, A. G. A., et al.  
2023, *A&A*, 674, A1, doi: [10.1051/0004-6361/202243940](https://doi.org/10.1051/0004-6361/202243940)
- Gallagher, J. S., Tolstoy, E., Dohm-Palmer, R. C., et al.  
1998, *AJ*, 115, 1869, doi: [10.1086/300328](https://doi.org/10.1086/300328)
- Gallart, C., Aparicio, A., Bertelli, G., & Chiosi, C. 1996,  
*AJ*, 112, 1950, doi: [10.1086/118154](https://doi.org/10.1086/118154)
- Gallart, C., Zoccali, M., & Aparicio, A. 2005, *ARA&A*, 43,  
387, doi: [10.1146/annurev.astro.43.072103.150608](https://doi.org/10.1146/annurev.astro.43.072103.150608)
- Gallart, C., Monelli, M., Mayer, L., et al. 2015, *ApJL*, 811,  
L18, doi: [10.1088/2041-8205/811/2/L18](https://doi.org/10.1088/2041-8205/811/2/L18)
- Geha, M., Weisz, D., Grocholski, A., et al. 2015, *ApJ*, 811,  
114, doi: [10.1088/0004-637X/811/2/114](https://doi.org/10.1088/0004-637X/811/2/114)
- Girardi, L. 2016, *ARA&A*, 54, 95,  
doi: [10.1146/annurev-astro-081915-023354](https://doi.org/10.1146/annurev-astro-081915-023354)
- Girardi, L., Groenewegen, M. A. T., Hatziminaoglou, E., &  
da Costa, L. 2005, *A&A*, 436, 895,  
doi: [10.1051/0004-6361:20042352](https://doi.org/10.1051/0004-6361:20042352)
- Girardi, L., Williams, B. F., Gilbert, K. M., et al. 2010,  
*ApJ*, 724, 1030, doi: [10.1088/0004-637X/724/2/1030](https://doi.org/10.1088/0004-637X/724/2/1030)
- Gogarten, S. M., Dalcanton, J. J., Williams, B. F., et al.  
2010, *ApJ*, 712, 858, doi: [10.1088/0004-637X/712/2/858](https://doi.org/10.1088/0004-637X/712/2/858)
- Gullieuszik, M., Held, E. V., Rizzi, L., et al. 2008a,  
*MNRAS*, 388, 1185,  
doi: [10.1111/j.1365-2966.2008.13400.x](https://doi.org/10.1111/j.1365-2966.2008.13400.x)
- Gullieuszik, M., Held, E. V., Rizzi, L., et al. 2007a, *A&A*,  
467, 1025, doi: [10.1051/0004-6361:20066788](https://doi.org/10.1051/0004-6361:20066788)
- Gullieuszik, M., Rejkuba, M., Cioni, M. R., Habing, H. J.,  
& Held, E. V. 2007b, *A&A*, 475, 467,  
doi: [10.1051/0004-6361:20066848](https://doi.org/10.1051/0004-6361:20066848)
- Gullieuszik, M., Greggio, L., Held, E. V., et al. 2008b,  
*A&A*, 483, L5, doi: [10.1051/0004-6361:200809631](https://doi.org/10.1051/0004-6361:200809631)
- Habel, N., Nally, C., Lenkić, L., et al. 2024, *ApJ*, 971, 108,  
doi: [10.3847/1538-4357/ad5343](https://doi.org/10.3847/1538-4357/ad5343)
- Hargis, J. R., Albers, S., Crnojević, D., et al. 2020, *ApJ*,  
888, 31, doi: [10.3847/1538-4357/ab58d2](https://doi.org/10.3847/1538-4357/ab58d2)
- Harmsen, B., Bell, E. F., D'Souza, R., et al. 2023, *MNRAS*,  
525, 4497, doi: [10.1093/mnras/stad2480](https://doi.org/10.1093/mnras/stad2480)
- Harris, C. R., Millman, K. J., van der Walt, S. J., et al.  
2020, *Nature*, 585, 357, doi: [10.1038/s41586-020-2649-2](https://doi.org/10.1038/s41586-020-2649-2)
- Harris, J., & Zaritsky, D. 2004, *AJ*, 127, 1531,  
doi: [10.1086/381953](https://doi.org/10.1086/381953)
- Harris, J., & Zaritsky, D. 2009, *AJ*, 138, 1243,  
doi: [10.1088/0004-6256/138/5/1243](https://doi.org/10.1088/0004-6256/138/5/1243)
- Held, E. V., Gullieuszik, M., Rizzi, L., et al. 2010, *MNRAS*,  
404, 1475, doi: [10.1111/j.1365-2966.2010.16358.x](https://doi.org/10.1111/j.1365-2966.2010.16358.x)
- Hidalgo, S. L., Aparicio, A., Skillman, E., et al. 2011, *ApJ*,  
730, 14, doi: [10.1088/0004-637X/730/1/14](https://doi.org/10.1088/0004-637X/730/1/14)
- Hidalgo, S. L., Monelli, M., Aparicio, A., et al. 2013, *ApJ*,  
778, 103, doi: [10.1088/0004-637X/778/2/103](https://doi.org/10.1088/0004-637X/778/2/103)
- Hidalgo, S. L., Pietrinferni, A., Cassisi, S., et al. 2018, *ApJ*,  
856, 125, doi: [10.3847/1538-4357/aab158](https://doi.org/10.3847/1538-4357/aab158)
- Hodge, P. W., Dolphin, A. E., Smith, T. R., & Mateo, M.  
1999, *ApJ*, 521, 577, doi: [10.1086/307595](https://doi.org/10.1086/307595)
- Holtzman, J. A., Afonso, C., & Dolphin, A. 2006, *ApJS*,  
166, 534, doi: [10.1086/507074](https://doi.org/10.1086/507074)
- Hunter, J. D. 2007, *Computing in Science & Engineering*, 9,  
90, doi: [10.1109/MCSE.2007.55](https://doi.org/10.1109/MCSE.2007.55)
- Huynh, K., Pastorelli, G., & Boyer, M. 2025, in *American  
Astronomical Society Meeting Abstracts*, Vol. 246, 246th  
Meeting of the American Astronomical Society, 406.06
- Jackson, D. C., Skillman, E. D., Cannon, J. M., & Côté, S.  
2004, *AJ*, 128, 1219, doi: [10.1086/423292](https://doi.org/10.1086/423292)
- Jackson, D. C., Skillman, E. D., Gehrz, R. D., Polomski,  
E., & Woodward, C. E. 2007, *ApJ*, 656, 818,  
doi: [10.1086/510354](https://doi.org/10.1086/510354)
- Jacobs, B. A., Rizzi, L., Tully, R. B., et al. 2009, *AJ*, 138,  
332, doi: [10.1088/0004-6256/138/2/332](https://doi.org/10.1088/0004-6256/138/2/332)
- Javadi, A., van Loon, J. T., & Mirtorabi, M. T. 2011a,  
*MNRAS*, 414, 3394,  
doi: [10.1111/j.1365-2966.2011.18638.x](https://doi.org/10.1111/j.1365-2966.2011.18638.x)
- Javadi, A., van Loon, J. T., & Mirtorabi, M. T. 2011b,  
*MNRAS*, 411, 263, doi: [10.1111/j.1365-2966.2010.17678.x](https://doi.org/10.1111/j.1365-2966.2010.17678.x)
- Jung, M. Y., Ko, J., Kim, J.-W., et al. 2012, *A&A*, 543,  
A35, doi: [10.1051/0004-6361/201219033](https://doi.org/10.1051/0004-6361/201219033)
- Kang, A., Sohn, Y.-J., Rhee, J., et al. 2005, *A&A*, 437, 61,  
doi: [10.1051/0004-6361:20052692](https://doi.org/10.1051/0004-6361:20052692)

- Kennicutt, R. C., & Evans, N. J. 2012, *ARA&A*, 50, 531, doi: [10.1146/annurev-astro-081811-125610](https://doi.org/10.1146/annurev-astro-081811-125610)
- Khademi, M., Yang, Y., Hammer, F., & Nasiri, S. 2021, *A&A*, 654, A7, doi: [10.1051/0004-6361/202140336](https://doi.org/10.1051/0004-6361/202140336)
- Koch, E. W., Leroy, A. K., Rosolowsky, E. W., et al. 2025, *ApJS*, 279, 35, doi: [10.3847/1538-4365/ade0ad](https://doi.org/10.3847/1538-4365/ade0ad)
- Kolhe, N., Hammer, F., Yang, Y., et al. 2026, arXiv e-prints, arXiv:2602.02652. <https://arxiv.org/abs/2602.02652>
- Kroupa, P. 2001, *MNRAS*, 322, 231, doi: [10.1046/j.1365-8711.2001.04022.x](https://doi.org/10.1046/j.1365-8711.2001.04022.x)
- Kruijssen, J. M. D., Pelupessy, F. I., Lamers, H. J. G. L. M., Portegies Zwart, S. F., & Icke, V. 2011, *MNRAS*, 414, 1339, doi: [10.1111/j.1365-2966.2011.18467.x](https://doi.org/10.1111/j.1365-2966.2011.18467.x)
- Krumholz, M. R., McKee, C. F., & Bland-Hawthorn, J. 2019, *ARA&A*, 57, 227, doi: [10.1146/annurev-astro-091918-104430](https://doi.org/10.1146/annurev-astro-091918-104430)
- Leaman, R., Cole, A. A., Venn, K. A., et al. 2009, *ApJ*, 699, 1, doi: [10.1088/0004-637X/699/1/1](https://doi.org/10.1088/0004-637X/699/1/1)
- Leaman, R., Venn, K. A., Brooks, A. M., et al. 2013, *ApJ*, 767, 131, doi: [10.1088/0004-637X/767/2/131](https://doi.org/10.1088/0004-637X/767/2/131)
- Lee, A. J., Freedman, W. L., Madore, B. F., et al. 2021, *ApJ*, 907, 112, doi: [10.3847/1538-4357/abd253](https://doi.org/10.3847/1538-4357/abd253)
- Lee, A. J., Weisz, D. R., Ren, Y., Savino, A., & Dolphin, A. E. 2025, *ApJ*, 995, 135, doi: [10.3847/1538-4357/ae12f0](https://doi.org/10.3847/1538-4357/ae12f0)
- Lee, H., Skillman, E. D., & Venn, K. A. 2005, *ApJ*, 620, 223, doi: [10.1086/427019](https://doi.org/10.1086/427019)
- Lee, M. G., Aparicio, A., Tikonov, N., Byun, Y.-I., & Kim, E. 1999, *AJ*, 118, 853, doi: [10.1086/300988](https://doi.org/10.1086/300988)
- Li, S., Riess, A. G., Scolnic, D., Casertano, S., & Anand, G. S. 2025, *ApJ*, 988, 97, doi: [10.3847/1538-4357/addd0c](https://doi.org/10.3847/1538-4357/addd0c)
- Marigo, P., Girardi, L., Bressan, A., et al. 2017, *ApJ*, 835, 77, doi: [10.3847/1538-4357/835/1/77](https://doi.org/10.3847/1538-4357/835/1/77)
- Martin, N. F., de Jong, J. T. A., & Rix, H.-W. 2008, *ApJ*, 684, 1075, doi: [10.1086/590336](https://doi.org/10.1086/590336)
- Martin, N. F., Ibata, R. A., Lewis, G. F., et al. 2016, *ApJ*, 833, 167, doi: [10.3847/1538-4357/833/2/167](https://doi.org/10.3847/1538-4357/833/2/167)
- Mateo, M. L. 1998, *ARA&A*, 36, 435, doi: [10.1146/annurev.astro.36.1.435](https://doi.org/10.1146/annurev.astro.36.1.435)
- Mazzi, A., Girardi, L., Zaggia, S., et al. 2021, *MNRAS*, 508, 245, doi: [10.1093/mnras/stab2399](https://doi.org/10.1093/mnras/stab2399)
- McConnachie, A. W. 2012, *AJ*, 144, 4, doi: [10.1088/0004-6256/144/1/4](https://doi.org/10.1088/0004-6256/144/1/4)
- McConnachie, A. W., Irwin, M. J., Ferguson, A. M. N., et al. 2005, *MNRAS*, 356, 979, doi: [10.1111/j.1365-2966.2004.08514.x](https://doi.org/10.1111/j.1365-2966.2004.08514.x)
- McKinney, W. 2010, in *Proceedings of the 9th Python in Science Conference*, ed. Stéfan van der Walt & Jarrod Millman, 56 – 61, doi: [10.25080/Majora-92bf1922-00a](https://doi.org/10.25080/Majora-92bf1922-00a)
- McQuinn, K. B. W., Skillman, E. D., Cannon, J. M., et al. 2010a, *ApJ*, 721, 297, doi: [10.1088/0004-637X/721/1/297](https://doi.org/10.1088/0004-637X/721/1/297)
- McQuinn, K. B. W., Skillman, E. D., Cannon, J. M., et al. 2010b, *ApJ*, 724, 49, doi: [10.1088/0004-637X/724/1/49](https://doi.org/10.1088/0004-637X/724/1/49)
- McQuinn, K. B. W., Boyer, M. L., Mitchell, M. B., et al. 2017, *ApJ*, 834, 78, doi: [10.3847/1538-4357/834/1/78](https://doi.org/10.3847/1538-4357/834/1/78)
- McQuinn, K. B. W., Newman, M. J. B., Skillman, E. D., et al. 2024a, *ApJ*, 976, 60, doi: [10.3847/1538-4357/ad8158](https://doi.org/10.3847/1538-4357/ad8158)
- McQuinn, K. B. W., B. Newman, M. J., Savino, A., et al. 2024b, *ApJ*, 961, 16, doi: [10.3847/1538-4357/ad1105](https://doi.org/10.3847/1538-4357/ad1105)
- Melbourne, J., Williams, B., Dalcanton, J., et al. 2010, *ApJ*, 712, 469, doi: [10.1088/0004-637X/712/1/469](https://doi.org/10.1088/0004-637X/712/1/469)
- Menzies, J., Feast, M., Whitelock, P., et al. 2008, *MNRAS*, 385, 1045, doi: [10.1111/j.1365-2966.2008.12907.x](https://doi.org/10.1111/j.1365-2966.2008.12907.x)
- Mercado, F. J., Bullock, J. S., Boylan-Kolchin, M., et al. 2021, *MNRAS*, 501, 5121, doi: [10.1093/mnras/staa3958](https://doi.org/10.1093/mnras/staa3958)
- Monelli, M., Hidalgo, S. L., Stetson, P. B., et al. 2010a, *ApJ*, 720, 1225, doi: [10.1088/0004-637X/720/2/1225](https://doi.org/10.1088/0004-637X/720/2/1225)
- Monelli, M., Gallart, C., Hidalgo, S. L., et al. 2010b, *ApJ*, 722, 1864, doi: [10.1088/0004-637X/722/2/1864](https://doi.org/10.1088/0004-637X/722/2/1864)
- Monelli, M., Martínez-Vázquez, C. E., Bernard, E. J., et al. 2016, *ApJ*, 819, 147, doi: [10.3847/0004-637X/819/2/147](https://doi.org/10.3847/0004-637X/819/2/147)
- Muñoz, R. R., Côté, P., Santana, F. A., et al. 2018, *ApJ*, 860, 66, doi: [10.3847/1538-4357/aac16b](https://doi.org/10.3847/1538-4357/aac16b)
- Nally, C., Jones, O. C., Lenkić, L., et al. 2024, *MNRAS*, 531, 183, doi: [10.1093/mnras/stae1163](https://doi.org/10.1093/mnras/stae1163)
- Newman, M. J. B., McQuinn, K. B. W., Skillman, E. D., et al. 2024, *ApJ*, 975, 195, doi: [10.3847/1538-4357/ad79f8](https://doi.org/10.3847/1538-4357/ad79f8)
- Nikolaev, S., & Weinberg, M. D. 2000, *ApJ*, 542, 804, doi: [10.1086/317048](https://doi.org/10.1086/317048)
- Pace, A. B. 2025, *The Open Journal of Astrophysics*, 8, 142, doi: [10.33232/001c.144859](https://doi.org/10.33232/001c.144859)
- Pastorelli, G., Marigo, P., Girardi, L., et al. 2019, *MNRAS*, 485, 5666, doi: [10.1093/mnras/stz725](https://doi.org/10.1093/mnras/stz725)
- Pastorelli, G., Marigo, P., Girardi, L., et al. 2020, *MNRAS*, 498, 3283, doi: [10.1093/mnras/staa2565](https://doi.org/10.1093/mnras/staa2565)
- Pedregosa, F., Varoquaux, G., Gramfort, A., et al. 2011, *Journal of Machine Learning Research*, 12, 2825, doi: [10.48550/arXiv.1201.0490](https://doi.org/10.48550/arXiv.1201.0490)
- Persson, S. E., Murphy, D. C., Smee, S., et al. 2013, *PASP*, 125, 654, doi: [10.1086/671164](https://doi.org/10.1086/671164)
- Portegies Zwart, S. F., McMillan, S. L. W., & Gieles, M. 2010, *ARA&A*, 48, 431, doi: [10.1146/annurev-astro-081309-130834](https://doi.org/10.1146/annurev-astro-081309-130834)
- Portegies Zwart, S. F., McMillan, S. L. W., Hut, P., & Makino, J. 2001, *MNRAS*, 321, 199, doi: [10.1046/j.1365-8711.2001.03976.x](https://doi.org/10.1046/j.1365-8711.2001.03976.x)
- Reid, N., & Mould, J. 1984, *ApJ*, 284, 98, doi: [10.1086/162388](https://doi.org/10.1086/162388)

- Rejkuba, M., Harris, W. E., Greggio, L., Crnojević, D., & Harris, G. L. H. 2022, *A&A*, 657, A41, doi: [10.1051/0004-6361/202141347](https://doi.org/10.1051/0004-6361/202141347)
- Richardson, J. C., Ferguson, A. M. N., Johnson, R. A., et al. 2008, *AJ*, 135, 1998, doi: [10.1088/0004-6256/135/6/1998](https://doi.org/10.1088/0004-6256/135/6/1998)
- Rubele, S., Girardi, L., Kerber, L., et al. 2015, *MNRAS*, 449, 639, doi: [10.1093/mnras/stv141](https://doi.org/10.1093/mnras/stv141)
- Rubele, S., Pastorelli, G., Girardi, L., et al. 2018, *MNRAS*, 478, 5017, doi: [10.1093/mnras/sty1279](https://doi.org/10.1093/mnras/sty1279)
- Sacchi, E., Cignoni, M., Aloisi, A., et al. 2018, *ApJ*, 857, 63, doi: [10.3847/1538-4357/aab844](https://doi.org/10.3847/1538-4357/aab844)
- Sacchi, E., Cignoni, M., Aloisi, A., et al. 2019, *ApJ*, 878, 1, doi: [10.3847/1538-4357/ab1de1](https://doi.org/10.3847/1538-4357/ab1de1)
- Sacchi, E., Richstein, H., Kallivayalil, N., et al. 2021, *ApJL*, 920, L19, doi: [10.3847/2041-8213/ac2aa3](https://doi.org/10.3847/2041-8213/ac2aa3)
- Sandage, A., & Carlson, G. 1985, *AJ*, 90, 1464, doi: [10.1086/113856](https://doi.org/10.1086/113856)
- Sarajedini, A. 2023, *MNRAS*, 521, 3847, doi: [10.1093/mnras/stad738](https://doi.org/10.1093/mnras/stad738)
- Savino, A., Tolstoy, E., Salaris, M., Monelli, M., & de Boer, T. J. L. 2019, *A&A*, 630, A116, doi: [10.1051/0004-6361/201936077](https://doi.org/10.1051/0004-6361/201936077)
- Savino, A., Weisz, D. R., Skillman, E. D., et al. 2023, *ApJ*, 956, 86, doi: [10.3847/1538-4357/acf46f](https://doi.org/10.3847/1538-4357/acf46f)
- Savino, A., Gennaro, M., Dolphin, A. E., et al. 2024, *ApJ*, 970, 36, doi: [10.3847/1538-4357/ad4e2f](https://doi.org/10.3847/1538-4357/ad4e2f)
- Savino, A., Weisz, D. R., Dolphin, A. E., et al. 2025, *ApJ*, 979, 205, doi: [10.3847/1538-4357/ada24f](https://doi.org/10.3847/1538-4357/ada24f)
- Schlafly, E. F., & Finkbeiner, D. P. 2011, *ApJ*, 737, 103, doi: [10.1088/0004-637X/737/2/103](https://doi.org/10.1088/0004-637X/737/2/103)
- Skillman, E. D., & Gallart, C. 2002, in *Astronomical Society of the Pacific Conference Series*, Vol. 274, *Observed HR Diagrams and Stellar Evolution*, ed. T. Lejeune & J. Fernandes, 535
- Skillman, E. D., Tolstoy, E., Cole, A. A., et al. 2003, *ApJ*, 596, 253, doi: [10.1086/377635](https://doi.org/10.1086/377635)
- Skillman, E. D., Hidalgo, S. L., Weisz, D. R., et al. 2014, *ApJ*, 786, 44, doi: [10.1088/0004-637X/786/1/44](https://doi.org/10.1088/0004-637X/786/1/44)
- Skillman, E. D., Monelli, M., Weisz, D. R., et al. 2017, *ApJ*, 837, 102, doi: [10.3847/1538-4357/aa60c5](https://doi.org/10.3847/1538-4357/aa60c5)
- Smercina, A., Bell, E. F., Williams, B. F., et al. 2025, *arXiv e-prints*, arXiv:2507.13349, doi: [10.48550/arXiv.2507.13349](https://doi.org/10.48550/arXiv.2507.13349)
- Sohn, Y.-J., Kang, A., Rhee, J., et al. 2006, *A&A*, 445, 69, doi: [10.1051/0004-6361:20053583](https://doi.org/10.1051/0004-6361:20053583)
- Stetson, P. B. 1987, *PASP*, 99, 191, doi: [10.1086/131977](https://doi.org/10.1086/131977)
- Stetson, P. B. 1994, *PASP*, 106, 250, doi: [10.1086/133378](https://doi.org/10.1086/133378)
- Stetson, P. B. 2011, *DAOPHOT: Crowded-field Stellar Photometry Package*, Astrophysics Source Code Library, record ascl:1104.011
- Taibi, S., Battaglia, G., Leaman, R., et al. 2022, *A&A*, 665, A92, doi: [10.1051/0004-6361/202243508](https://doi.org/10.1051/0004-6361/202243508)
- Tang, J., Bressan, A., Rosenfield, P., et al. 2014, *MNRAS*, 445, 4287, doi: [10.1093/mnras/stu2029](https://doi.org/10.1093/mnras/stu2029)
- Tolstoy, E., Hill, V., & Tosi, M. 2009, *ARA&A*, 47, 371, doi: [10.1146/annurev-astro-082708-101650](https://doi.org/10.1146/annurev-astro-082708-101650)
- Urbaneja, M. A., Kudritzki, R.-P., Bresolin, F., et al. 2008, *ApJ*, 684, 118, doi: [10.1086/590334](https://doi.org/10.1086/590334)
- Valcheva, A. T., Ivanov, V. D., Ovcharov, E. P., & Nedialkov, P. L. 2007, *A&A*, 466, 501, doi: [10.1051/0004-6361:20054536](https://doi.org/10.1051/0004-6361:20054536)
- Velguth, B. N., Bell, E. F., Smercina, A., et al. 2024, *ApJ*, 974, 189, doi: [10.3847/1538-4357/ad6cd8](https://doi.org/10.3847/1538-4357/ad6cd8)
- Venn, K. A., Tolstoy, E., Kaufer, A., et al. 2003, *AJ*, 126, 1326, doi: [10.1086/377345](https://doi.org/10.1086/377345)
- Weisz, D. R., Dolphin, A. E., Skillman, E. D., et al. 2014a, *ApJ*, 789, 148, doi: [10.1088/0004-637X/789/2/148](https://doi.org/10.1088/0004-637X/789/2/148)
- Weisz, D. R., Dolphin, A. E., Skillman, E. D., et al. 2014b, *ApJ*, 789, 147, doi: [10.1088/0004-637X/789/2/147](https://doi.org/10.1088/0004-637X/789/2/147)
- Weisz, D. R., Skillman, E. D., Cannon, J. M., et al. 2008, *ApJ*, 689, 160, doi: [10.1086/592323](https://doi.org/10.1086/592323)
- Weisz, D. R., Dalcanton, J. J., Williams, B. F., et al. 2011, *ApJ*, 739, 5, doi: [10.1088/0004-637X/739/1/5](https://doi.org/10.1088/0004-637X/739/1/5)
- Weisz, D. R., McQuinn, K. B. W., Savino, A., et al. 2023, *ApJS*, 268, 15, doi: [10.3847/1538-4365/acdcfd](https://doi.org/10.3847/1538-4365/acdcfd)
- Weisz, D. R., Dolphin, A. E., Savino, A., et al. 2024, *ApJS*, 271, 47, doi: [10.3847/1538-4365/ad2600](https://doi.org/10.3847/1538-4365/ad2600)
- Williams, B. F., Dalcanton, J. J., Seth, A. C., et al. 2009, *AJ*, 137, 419, doi: [10.1088/0004-6256/137/1/419](https://doi.org/10.1088/0004-6256/137/1/419)
- Williams, B. F., Dalcanton, J. J., Stilp, A., et al. 2010, *ApJ*, 709, 135, doi: [10.1088/0004-637X/709/1/135](https://doi.org/10.1088/0004-637X/709/1/135)
- Williams, B. F., Dolphin, A. E., Dalcanton, J. J., et al. 2017, *ApJ*, 846, 145, doi: [10.3847/1538-4357/aa862a](https://doi.org/10.3847/1538-4357/aa862a)
- Wood, P. R., Bessell, M. S., & Paltoglou, G. 1985, *ApJ*, 290, 477, doi: [10.1086/163005](https://doi.org/10.1086/163005)
- Zijlstra, A. A., Loup, C., Waters, L. B. F. M., et al. 1996, *MNRAS*, 279, 32, doi: [10.1093/mnras/279.1.32](https://doi.org/10.1093/mnras/279.1.32)